

Review

Graphene-Based Electrochemical Nano-Biosensors for Detection of SARS-CoV-2

Joydip Sengupta ¹ and Chaudhery Mustansar Hussain ^{2,*}¹ Department of Electronic Science, Jogesh Chandra Chaudhuri College, Kolkata 700033, India² Department of Chemistry and Environmental Science, New Jersey Institute of Technology, Newark, NJ 07102, USA* Correspondence: chaudhery.m.hussain@njit.edu

Abstract: COVID-19, a viral respiratory illness, is caused by Severe Acute Respiratory Syndrome Corona Virus 2 (SARS-CoV-2), which was first identified in Wuhan, China, in 2019 and rapidly spread worldwide. Testing and isolation were essential to control the virus's transmission due to the severity of the disease. In this context, there is a global interest in the feasibility of employing nano-biosensors, especially those using graphene as a key material, for the real-time detection of the virus. The exceptional properties of graphene and the outstanding performance of nano-biosensors in identifying various viruses prompted a feasibility check on this technology. This paper focuses on the recent advances in using graphene-based electrochemical biosensors for sensing the SARS-CoV-2 virus. Specifically, it reviews various types of electrochemical biosensors, including amperometric, potentiometric, and impedimetric biosensors, and discusses the current challenges associated with biosensors for SARS-CoV-2 detection. The conclusion of this review discusses future directions in the field of electrochemical biosensors for SARS-CoV-2 detection, underscoring the importance of continued research and development in this domain.

Keywords: SARS-CoV-2; graphene; electrochemistry; biosensor; COVID-19; virus detection; amperometric biosensors; potentiometric biosensors; impedimetric biosensors; biomarkers



Citation: Sengupta, J.; Hussain, C.M. Graphene-Based Electrochemical Nano-Biosensors for Detection of SARS-CoV-2. *Inorganics* **2023**, *11*, 197. <https://doi.org/10.3390/inorganics11050197>

Academic Editors: Antonino Gulino and Zuzana Vlckova Zivcova

Received: 28 January 2023

Revised: 13 April 2023

Accepted: 28 April 2023

Published: 1 May 2023



Copyright: © 2023 by the authors. Licensee MDPI, Basel, Switzerland. This article is an open access article distributed under the terms and conditions of the Creative Commons Attribution (CC BY) license (<https://creativecommons.org/licenses/by/4.0/>).

1. Introduction

1.1. SARS-CoV-2 and Biosensors

SARS-CoV-2 is the virus that causes COVID-19. It is a member of the coronavirus family, which also includes SARS-CoV and MERS-CoV. The epidemiology of SARS-CoV-2 continues to evolve as more is learned about the virus and its transmission. Monitoring cases and implementing public health measures to prevent the spread of the virus remain key components for controlling the COVID-19 pandemic. Some key epidemiological features of SARS-CoV-2 are outlined below.

- **Transmission:** SARS-CoV-2 is primarily transmitted through respiratory droplets when an infected person coughs, sneezes, or talks [1]. The virus can also be spread by touching a surface contaminated with the virus and then touching one's face. Airborne transmission is also possible in certain settings, particularly enclosed spaces with poor ventilation [2].
- **Incubation period:** The incubation period for SARS-CoV-2 ranges from 2 to 14 days, with an average of 5 to 6 days. However, some people may develop symptoms outside of this range [3].
- **Symptoms:** The most common symptoms of COVID-19 include fever, cough, and shortness of breath. Other symptoms may include fatigue, body aches, headache, loss of smell or taste, sore throat, congestion, and runny nose. Some people may be asymptomatic, meaning they do not have any symptoms.

- **Severity:** COVID-19 can range in severity from mild to severe illness and can be fatal in some cases. Older adults and people with underlying health conditions, such as diabetes, obesity, heart disease, or weakened immune systems, are at a higher risk for severe illness and death [4].
- **Case fatality rate:** The case fatality rate (CFR) for COVID-19 varies by age and underlying health conditions. The overall global CFR has been estimated to be around 0.9% as of February 2023 [5].
- **Variants:** SARS-CoV-2 has mutated over time, leading to the emergence of several variants of concern (VOCs) and variants of interest (VOIs). VOCs include the Alpha, Beta, Gamma, and Delta variants, which are believed to be more transmissible and potentially more severe than the original strain of the virus. VOIs include several other variants with mutations that may impact transmission, severity, or immune response [6].
- **Global impact:** Since the start of the pandemic, COVID-19 has spread to virtually every country in the world, causing significant morbidity and mortality (Figure 1). As of 17 March 2023, there have been over 760 million confirmed cases and over 6.8 million deaths reported globally [5]. The impact of the pandemic has also had significant economic and social consequences, including disruptions to healthcare systems, education, and employment [7].

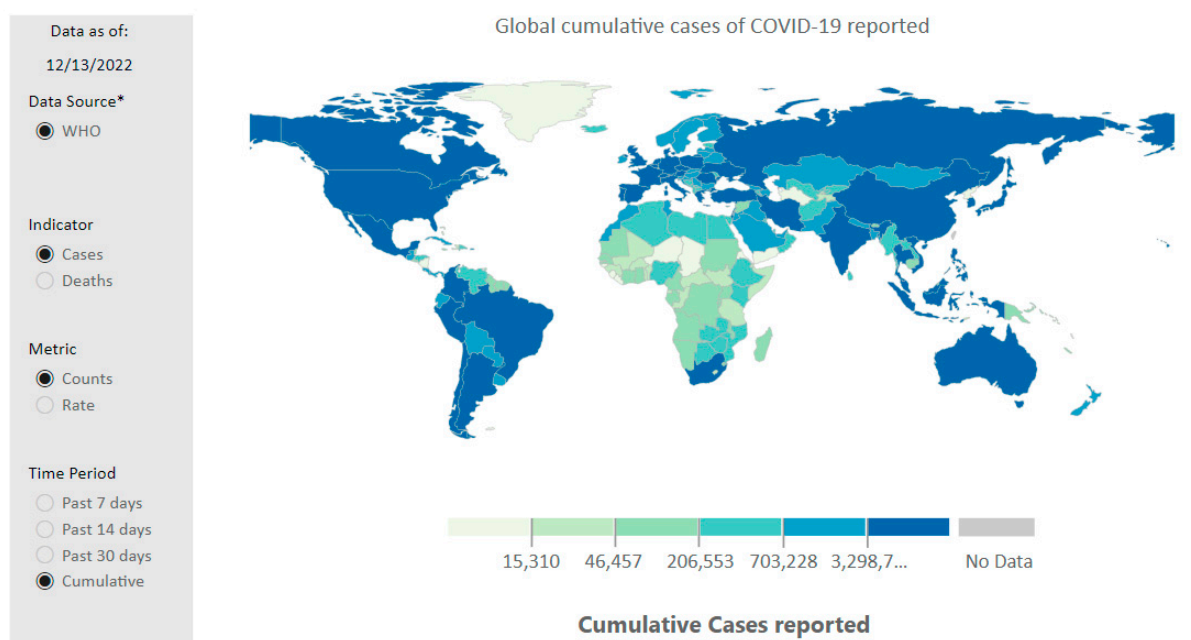


Figure 1. Global cumulative cases of COVID-19 (Reproduced with permission from [8]).

Structurally, SARS-CoV-2 is a single-stranded, positive-sense RNA virus that belongs to the coronavirus family. It is approximately 120–160 nm in diameter and has a characteristic “corona” or crown-like appearance due to the presence of spike proteins on its surface. These spike proteins bind to ACE2 receptors in human cells, allowing the virus to enter and infect the host cell. The virus is enclosed in a lipid bilayer envelope, which is derived from the host cell’s membrane. The envelope contains spike proteins and other viral proteins that play a role in viral replication and host cell entry [9]. The viral genome is approximately 30 kilobases in length and encodes for several structural and non-structural proteins (Table 1), including the spike protein, the envelope protein, the membrane protein, the nucleocapsid protein, and the viral enzymes required for replication (such as the protease and the RNA-dependent RNA polymerase) (Figure 2). Once the virus enters the host cell, it uses the host’s cellular machinery to replicate and produce new viral particles. It also suppresses the host’s immune response to enable its replication [10].

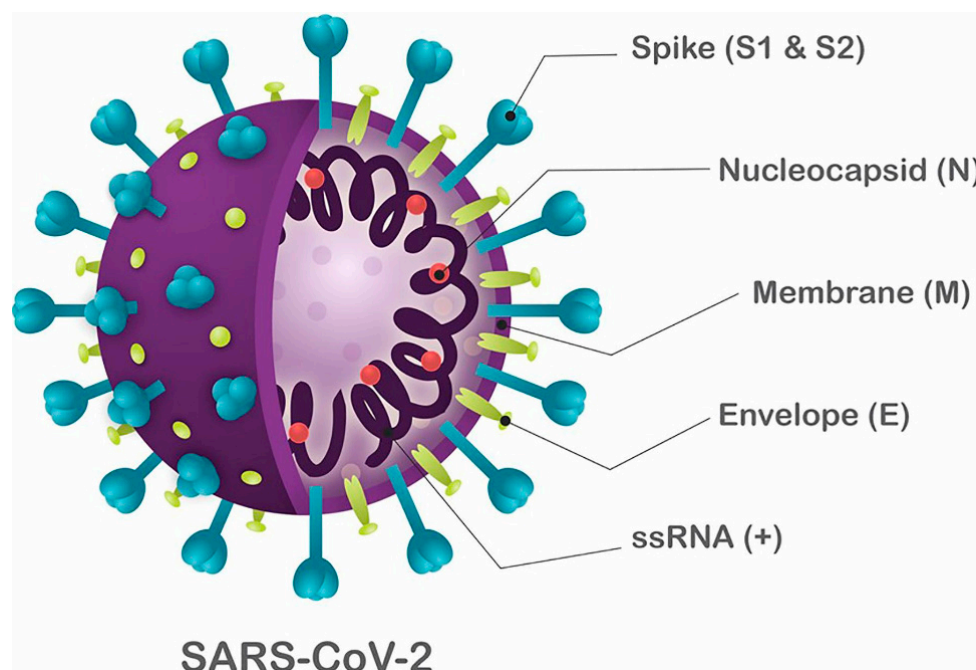


Figure 2. The basic framework of SARS-CoV-2 consists mainly of structural proteins, including spike (S), membrane (M), envelope (E), and nucleocapsid (N). The envelope is composed of a lipid bilayer that originates from the host cell membrane and encases the S, M, and E proteins. The N protein interacts with the viral RNA located at the center of the virion. (Reprinted with permission from [11]).

Table 1. The function of the structural proteins of SARS-CoV-2 (Reprinted with permission from [12]).

Protein	Function
Spike (S)	Binds and fuse to the host cell receptor and induces infection and transmission.
Nucleocapsid (N)	Binding to the viral RNA genome is critical for viral replication and genome packaging.
Membrane (M)	Viral assembly and shaping viral envelope.
Envelope (E)	Formation of the viral envelope.

The COVID-19 pandemic caused by the SARS-CoV-2 virus has highlighted the critical need for rapid and accurate diagnostic tools. Traditional methods for diagnosing viral infections, such as PCR and ELISA, have been widely used, but they have limitations in terms of cost, complexity, and turnaround time [13]. Biosensors offer a promising alternative for the rapid and sensitive detection of SARS-CoV-2 [14]. Biosensors are devices that combine biological recognition elements, such as antibodies or nucleic acids, with a transducer to convert the biological signal into a measurable signal. The development of novel biosensors for SARS-CoV-2 detection has several advantages over traditional methods. These include:

- **Rapid detection:** Biosensors can provide results in minutes or even seconds, which is crucial for timely diagnosis and treatment.
- **High sensitivity:** Biosensors can detect very low concentrations of the virus, which is important for early detection and surveillance.
- **Low cost:** Biosensors can be produced at a lower cost than traditional methods, making them more accessible in resource-limited settings.
- **Portable:** Biosensors can be designed to be portable, allowing for point-of-care testing in remote or underserved areas.
- **Non-invasive:** Biosensors can detect the virus from various sources, including saliva, urine, and breath, without the need for invasive sampling methods.

In the case of SARS-CoV-2, biosensors can be used to detect the virus in various samples, including respiratory samples (e.g., nasopharyngeal swabs), blood, and urine. There

are different types of biosensors that are capable of detecting SARS-CoV-2, such as optical biosensors [15], electrochemical biosensors [16], piezoelectric biosensors [17], thermal biosensors [18], magnetic biosensors [19], acoustic biosensors [20]. Among these, one of the most common types of biosensors used for SARS-CoV-2 detection is the electrochemical biosensor. These biosensors can use antibodies or nucleic acids specific to SARS-CoV-2 to detect the presence of the virus in a sample. They have high sensitivity and specificity and can provide results relatively quickly [21,22]. Biosensors can provide a rapid, easy-to-use, and cost-effective alternative to traditional diagnostic methods and are being developed to detect SARS-CoV-2 in various settings, including hospitals, laboratories, and point-of-care settings [23]. Nanomaterials, especially carbon nanomaterials in particular [24], have shown considerable potential for improving biosensor performance [25].

1.2. Graphene in Biosensor

Graphene is a two-dimensional material that consists of a single layer of carbon atoms arranged in a hexagonal lattice. Graphene is highly sensitive towards the detection of biological recognition elements because of its unique properties such as:

- High surface area and conductivity allow efficient capture and transduction of biomolecular interactions [26].
- High optical transparency and tunability enable optical sensing methods such as fluorescence, Raman scattering, and plasmon resonance [27].
- High mechanical flexibility and stability enable the fabrication of various device architectures, such as crumpled graphene or graphene nanoribbons [28].

Compared to other sensing materials such as gold, silicon, or carbon nanotubes, graphene has advantages such as lower cost, higher sensitivity, faster response time, and better biocompatibility [29]. Graphene has been extensively studied in the development of electrochemical biosensors due to its unique properties. Graphene-based electrochemical biosensors have been used for the detection of various biomolecules such as glucose [30], dopamine [31], cholesterol [32], nucleic acids [33], enzymes [34], proteins [35], etc. The detection mechanism of these biosensors is based on the immobilization of biomolecules on the graphene surface, which leads to a change in the electrical properties of graphene upon the binding of the target analyte. One of the most common strategies for the immobilization of biomolecules on graphene is the covalent functionalization of graphene [36] with reactive groups such as carboxylic acids [37], amines [38], and thiols [39]. The functionalized graphene can then be used to immobilize biomolecules through covalent bonding or physical adsorption. Another approach for the development of graphene-based biosensors is the use of graphene oxide (GO), which is a derivative of graphene. GO has hydrophilic functional groups such as carboxylic acid and hydroxyl groups, which makes it easy to disperse in aqueous solutions [40]. GO can be easily functionalized with biomolecules through non-covalent interactions such as π - π stacking and electrostatic interactions [41]. Overall, graphene-based electrochemical biosensors have shown great potential in the field of biosensing [42] (Figure 3).

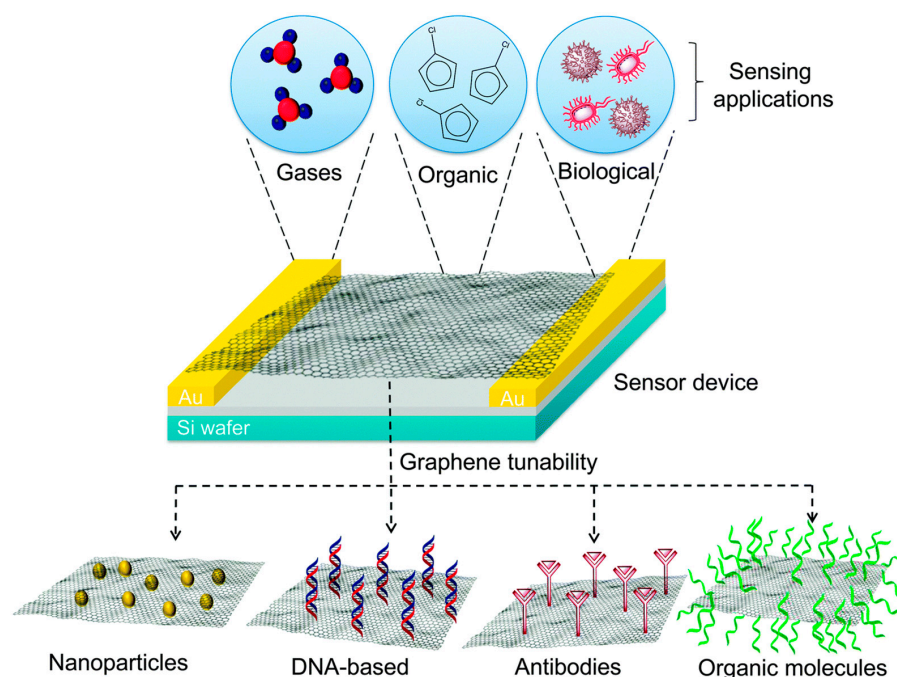


Figure 3. This diagram depicts a didactical plan for showcasing how a graphene-based sensor could function as a versatile detection platform for a range of substances, such as gases, organic molecules, microbial cells, and biomolecules. By immobilizing metallic nanoparticles, DNA, antibodies, and polymeric compounds on the surface of the graphitic materials, the sensitivity of the graphene-based electrodes can be fine-tuned to suit specific detection requirements (Reprinted with permission from [43]).

Thus, graphene-based electrochemical biosensors have been extensively employed for the detection of SARS-CoV-2. These biosensors typically use pristine graphene, graphene oxide (GO), or reduced graphene oxide (rGO) as the sensing material. They can be functionalized with specific antibodies that bind to the viral proteins [44], such as the nucleocapsid protein or the spike protein, which are found on the surface of the virus (Figure 4).

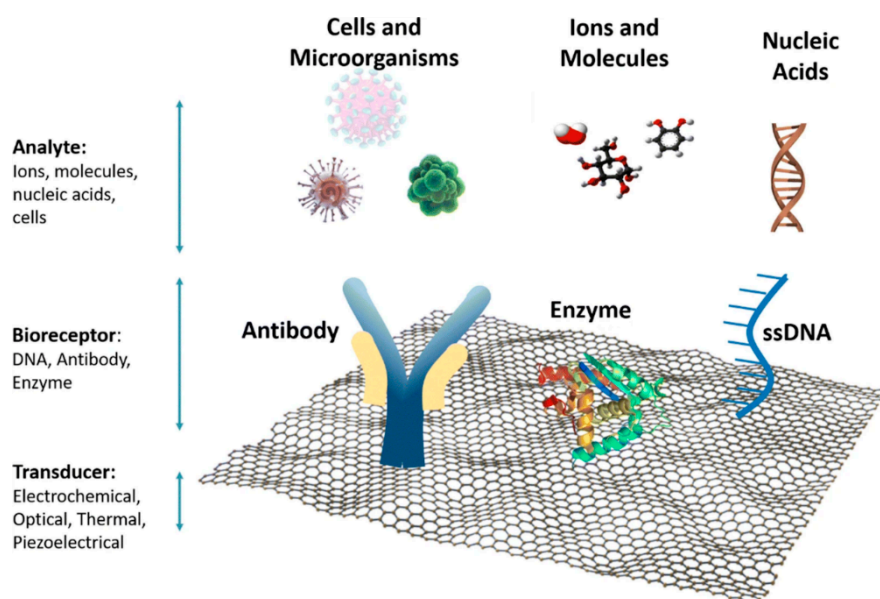


Figure 4. The primary components of a graphene-based biosensor. (Reprinted with permission from [45]).

In electrochemical biosensors, the functionalized graphene is used as a working electrode, and the sensor is completed upon referencing and a counter electrode [33]. The presence of the virus in a sample can be detected by measuring the change in current at the working electrode caused by the binding of the viral proteins to the antibodies on the graphene surface.

The high surface area and excellent electrical conductivity of graphene make it an attractive material for use in electrochemical biosensors [46]. These biosensors are a highly sensitive, selective, and rapid method for the detection of SARS-CoV-2 [47]. Additionally, graphene-based biosensors can be integrated with microfluidic devices for sample preparation and manipulation, which can further enhance the sensitivity and specificity of the biosensors [48].

In addition, graphene-based biosensors can also be integrated with other detection techniques, such as Raman spectroscopy or surface-enhanced Raman spectroscopy (SERS), to detect viral proteins. In these biosensors, the binding of the viral proteins to the antibodies on the graphene surface results in a change in the Raman signals that can be used to quantitatively or qualitatively detect the presence of the virus in the sample [49]. Overall, graphene-based biosensors have the potential to be a highly sensitive, selective, and rapid method for the detection of SARS-CoV-2 [50].

2. Electrochemical Biosensors for the Detection of SARS-CoV-2

An electrochemical biosensor is a type of biosensor that uses an electrode to detect the presence of a specific biomolecule, such as the SARS-CoV-2 virus. Electrochemical biosensors work by immobilizing specific biomolecules, such as antibodies or nucleic acids, on the surface of an electrode [51]. When the target biomolecule, such as the SARS-CoV-2 virus, is present in a sample, it binds to the immobilized biomolecules on the electrode surface. This binding causes a change in the electrical properties of the electrode, which can be measured and used to detect the presence of the virus. Electrochemical biosensors can provide rapid results and have high sensitivity and specificity for detecting SARS-CoV-2, making them a promising tool for COVID-19 diagnostics. The reaction under examination would typically create a quantifiable current (amperometric), a measurable potential or charge buildup (potentiometric), or a measurable impedance (impedimetric). The pros and cons of different types of electrochemical biosensors are listed in Table 2.

Table 2. Pros and cons of different types of electrochemical biosensors.

Biosensor Type	Pros	Cons
Amperometric	High sensitivity, low detection limit, and fast response time	Requires a high potential to operate, susceptible to interference from other electroactive species, may suffer from electrode fouling and drift over time, may require a redox mediator
Potentiometric	Low cost, easy to use, and good stability, suitable for continuous real-time monitoring,	Limited sensitivity, slow response time, large sensor size, high cost, the signal can be affected by pH and temperature changes
Impedimetric	High sensitivity, low detection limit, fast response time, good specificity, ability to detect changes in interfacial properties	Requires complex instrumentation, lower sensitivity compared to amperometric and potentiometric biosensors, can be affected by variations in solution conductivity, may require additional instrumentation for measurement, may require specialized surface functionalization

It is important to note that the advantages and limitations listed here are not exhaustive and may vary depending on the specific application and the desired performance characteristics. Furthermore, the choice of biosensor type will depend on various factors, including the target analyte, the sample matrix, and the intended use case for SARS-CoV-2 detection.

2.1. Amperometric Biosensors for the Detection of SARS-CoV-2

Amperometric biosensors are a type of biosensor that uses an electrochemical technique called amperometry to detect analytes of interest. In the case of SARS-CoV-2, amperometric biosensors can be used to detect the viral antigen or antibodies in a sample. These biosensors are used to measure the current generated by the oxidation or reduction of the analyte at the working electrode [52]. Here, the biosensor surface is altered with antibodies or antigens that attach to SARS-CoV-2 proteins for detection. When the biosensor interacts with a sample containing the virus, a shift in current at the working electrode occurs, indicating the presence of the virus [53].

2.1.1. Using Graphene

For the fast, facile, and remote evaluation of SARS-CoV-2 biomarkers (antigen, antibodies, and C-reactive protein) through the analysis of COVID-19 patient blood and saliva samples, Rodríguez et al. [54] used laser-engraved graphene (LSG) to create an affordable ultrasensitive portable telemedicine electrochemical platform (Figure 5). The SARS-CoV-2 RapidPlex boasts a range of features that make it an attractive testing option for COVID-19. These features include high sensitivity, low cost, ultra-fast detection, wireless remote capabilities, and multiplexed sensing, which can provide valuable information on three important aspects of the disease: viral infection (NP), immune response (IgG and IgM), and disease severity (CRP). The tasks were accomplished by binding individual receptors to the graphene surface through covalent bonding. To attach the necessary receptors to the graphene layer, pyrenebutyric acid (PBA) was utilized as a linker. The LOD values of these three biomarkers are as follows: for nucleocapsid protein, LODs were 0.1 $\mu\text{g}/\text{mL}$ (serum) and 0.5 ng/mL (saliva). For S1-IgG LODs were 2 $\mu\text{g}/\text{mL}$ (serum) and 0.2 $\mu\text{g}/\text{mL}$ (saliva), for S1-IgM LODs were 20 $\mu\text{g}/\text{mL}$ (serum) and 0.6 $\mu\text{g}/\text{mL}$ (saliva), and for CRP LODs were 10 $\mu\text{g}/\text{mL}$ (serum) and 0.1 $\mu\text{g}/\text{mL}$ (saliva).

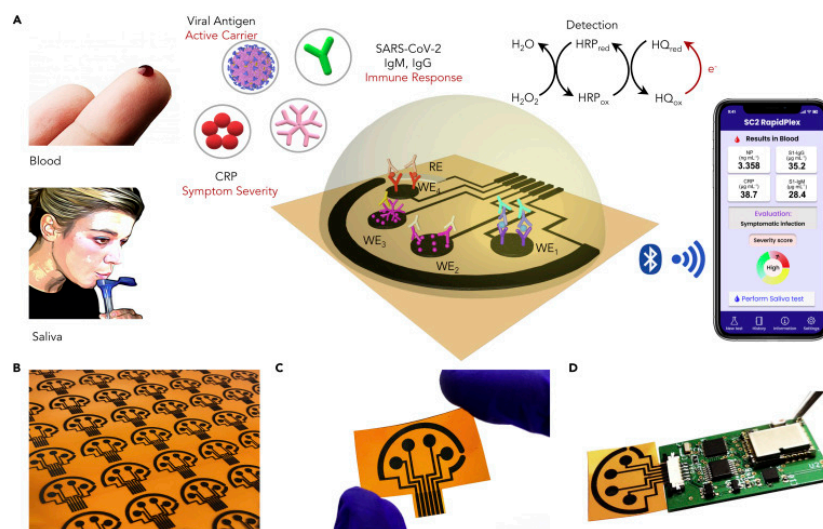


Figure 5. The SARS-CoV-2 RapidPlex is a telemedicine platform based on wireless graphene technology that can quickly and simultaneously detect SARS-CoV-2 in blood and saliva using multiple electrochemical sensors. (A) The figure depicts the SARS-CoV-2 RapidPlex multisensor telemedicine platform, which utilizes multiple sensors to detect SARS-CoV-2 viral proteins, as well as IgG and IgM antibodies and the inflammatory biomarker C-reactive protein (CRP). The platform is capable of wirelessly transmitting data to a mobile user interface. The working electrode (WE), counter electrode (CE), and reference electrode (RE) are essential components in the detection process. (B) Graphene sensor arrays are capable of mass production through laser engraving. (C) A picture of a flexible and disposable array made of graphene. (D) A visual depiction of the SARS-CoV-2 RapidPlex system, in which a graphene sensor array is connected to a printed circuit board to enable signal processing and wireless communication. (Reprinted with permission from [54]).

For improved immobilization of the plant-based anti-SARS-CoV-2 monoclonal antibody CR3022 (*Nicotiana benthamiana*), cellulose nanocrystals were adhered to screen-printed graphene electrodes. The modification resulted in an increased presence of COOH functional groups on the surface of the electrode, which was found to enhance the ability of the electrode to immobilize antibodies to a significant extent. The presence of the SARS-CoV-2 receptor binding domain (RBD) was then quantified by Jaewjaroenwattana et al. [55] using differential pulse voltammetry (DPV) by observing the changing current of a $[\text{Fe}(\text{CN})_6]^{3-/4-}$ redox solution with a LOD value of 2.0 fg/mL. The suggested electrochemical paper-based device could be effectively used to identify SARS-CoV-2 from nasopharyngeal swabs and saliva samples.

Ali et al. [56] employed aerosol jet 3D printing to create a reusable microfluidic biosensor with an array of 3D micro-length-scale electrode architecture. An intermediary layer of nano-graphene was used to coat the Au micropillar array, and the resulting structure was immobilized with N proteins utilizing EDC: NHS chemistry-based covalent conjugation before it was finally combined with a microfluidic channel. The designed electrochemical cell could detect SARS-CoV-2 antibodies to the N protein in seconds by monitoring antibody-antigen interaction. High sensitivity and a low LOD (13 fM) were established by the 3D electrode array because it minimizes the diffusion length for the electrochemical cell with radial ionic species diffusion.

To diagnose COVID-19, Beduk et al. [57] created a Laser-scribed graphene-based (LSG) electrochemical sensing system using 3D Au nanostructures to incorporate electroactive groups into an Au-modified LSG surface, where cysteamine and EDC: NHS were used as cross-linking agents. COOH groups on the electrode surface could covalently bind with amino-functionalized biorecognition elements, enabling the immobilization of carboxylic-rich anti-spike protein antibodies. Bovine serum albumin (BSA) was used to stabilize sensing performance in complex matrixes by preventing nonspecific interactions before spike protein detection. Following the appropriate surface modifications, this electrode was treated with the SARS-CoV-2 spike protein antibody. Due to its simplicity of use, accessibility, and organized data management, the smart antibody sensor was subsequently combined into a portable POC detection device that could be supervised by a customized smartphone application.

The 1-pyrene butyric acid N-hydroxysuccinimide ester (PBASE) linker was used to functionalize the graphene working electrode by Mojsoska et al. [58] to attach SARS-CoV-2 spike-specific antibodies. To establish the detection of the spike protein, the immunosensor surface was subjected to increasing antigen concentrations, and the resulting absolute change in the $[\text{Fe}(\text{CN})_6]^{3-/4-}$ current was measured. Only the SARS-CoV-2 spike protein could bind to the antibodies once the sample was added. The objective of the immunosensor was to identify signal alterations that result from SARS-CoV-2 antigen binding during a 45 min incubation period, and the resultant LOD was 260 nM.

To precisely detect the Delta variant of SARS-CoV-2, Yang et al. [59] developed a biosensor using graphene/chitosan as a substrate, which resulted in a high specific surface area and carrier mobility. The sensor was designed to immobilize sgRNA/dCas9 (dRNP) on its substrate to enable specific binding to the target nucleic acid of the SARS-CoV-2 Delta variant (Delta). The presence of sgRNA and the protospacer adjacent motif (PAM) site facilitated the binding process. The interaction between dRNP and the target DNA was responsible for the change in the electrochemical current signal, which was further amplified using the embedded electrochemical probe $[\text{Ru}(\text{Phen})_2\text{dppz}]\text{BF}_4$. Among other variations of SARS-CoV-2 (Alpha, Beta, and Gamma), the biosensor was able to specifically recognize Delta with a LOD of 1.2 pM.

For quick, accurate, label- and amplification-free SARS-CoV-2 detection, a graphene electrode was integrated into a flexible printed circuit board (PCB) by Damiati et al. [60]. To demonstrate the concept, a synthetic DNA strand matching the viral RNA sequence was detected using a two-step procedure that involved immobilization of a biotinylated complementary sequence on a surface modified with streptavidin, subsequently hybridization

with the target sequence and recording the result using the DPV technique with a LOD of 100 fg/mL in the presence of a ferro/ferricyanide redox couple.

Ji et al. [61] created a graphene microelectrode-based self-actuated molecular-electrochemical system (MECS) containing a tentacle and a trunk, both made of DNA nanostructure for the detection of SARS-CoV-2 viral RNA. To optimize biorecognition and prevent pseudo-signal, the probe and electrochemical label on the tentacle remained upright. In the presence of targeted nucleic acids, the adjacent tentacles spontaneously modify their shape, producing electrochemical responses with a LOD of 0.025 copies/ μ L.

A facile, non-enzymatic electrochemical sensor for the detection of SARS-CoV-2 cDNA was developed by Silva et al. [62] using a disposable, low-cost graphene polylactic (G-PLA) 3D-printed electrode modified with Au nanoparticles. Through a complex reaction with creatinine, the Au nanoparticles that were deposited on the electrode facilitated a reduction in the analytical response, leading to the development of a fast and straightforward electroanalytical device. This sensor was based on the immobilization of a viral cDNA capture sequence onto the reformed electrode and could detect viral cDNA at a level of 0.30 μ mol/L.

Tabrizi et al. [63] electrochemically produced a nanoporous anodic aluminum oxide membrane (NPAOM), then modified it with 3-mercaptopropyl trimethoxysilane (NPAOM-Si-SH) and decorated it with Au nanoparticles using Au ions and sodium borohydride. The resulting NPAOM-Si-S-Au_{nano} was affixed to the surface of a laser-engraved graphene electrode (LEGE) and placed inside a 3D-printed flow cell. Finally, a thiolated aptamer was introduced into the flow cell using a pump. The sensor's electrochemical performance was studied using square wave voltammetry (SWV), and its response to different concentrations of SARS-CoV-2-RBD was assessed within an environment containing potassium ferrocyanide acting as a redox probe. The sensor's detection limit was found to be 0.8 ng/mL, and it exhibited good selectivity for SARS-CoV-2-RBD even in the presence of other interfering agents in the human saliva sample.

An aptasensor was created by Tabrizi et al. [64] to identify the RBD of the SARS-CoV-2 virus using methylene blue (MB) encapsulated in a mesoporous silica film (MPSF). Amino-functionalized MPSF was electrochemically synthesized on the LEGE surface using silicon precursor and a template molecule (cetyltrimethylammonium bromide). The template was removed to encapsulate MB inside the MPSF (MB@MPSF). Finally, aptamer probes were immobilized on the MPSF surface to selectively interact with SARS-CoV-2-RBD, forming the aptasensor. When the virus was present, aptamers with a strong attraction to the virus were removed from the electrode surface to bind to the virus. The electrical signal was measured using SWV in saliva samples, with a detection limit of 0.36 ng/mL. The aptasensor exhibited high selectivity for detecting 32 ng/mL SARS-CoV-2-RBD in the presence of C-reactive protein, hemagglutinin, and neuraminidase of influenza A virus, as demonstrated by selectivity factor values of 35.9, 11.7, and 17.37, respectively.

For the rapid detection of COVID-19, an electrochemical sensor was developed by Primpray et al. [65] employing a graphene screen-printed electrode (GSPE) that was modified with poly (pyrrole propionic acid) because of its high carboxyl group content, which was needed for covalent binding with the SARS-CoV-2 RBD antibody. By competing with the capturing antibody for binding to the HRP-conjugated SARS-CoV-2 antigen, the SARS-CoV-2 RBD protein reduced the electrochemical current signal, allowing SARS-CoV-2 to be detected. The procedure employed a competitive enzyme immunoassay approach using SARS-CoV-2 coupled to horseradish peroxidase as a reporter binding molecule, which competes with the binding of an antibody against the SARS-CoV-2 receptor binding domain protein. The measurements produced a linear range of 0.01–1500 ng/mL, with low detection limits of 2 pg/mL and low quantification limits of 10 pg/mL.

2.1.2. Using Graphene Oxide

Kumar et al. [66] developed a bioreceptor based on peptides from human angiotensin-converting enzyme-2 (hACE-2) and utilized it to detect the SARS-CoV-2 spike protein

RBD. By adding MB electro-adsorbed GO to disposable carbon-SPE, they developed a platform for SARS-CoV-2 detection that is both inexpensive and readily scalable. Cyclic voltammetry (CV) and chronoamperometry (CA) were used to determine the concentration of spike proteins with minimum detection levels as low as 0.58 pg/mL and 0.71 pg/mL, respectively, in nasal/oral swab samples.

For the determination of SARS-CoV-2 spike protein, integration of bovine serum albumin and SARS-CoV-2 spike antibody in either a functionalized GO-modified glassy carbon electrode (BSA/AB/f-GO/GCE) or a screen-printed electrode (BSA/AB/f-GO/SPE) were used by Liv et al. [67]. Both the BSA/AB/f-GO/SPE and BSA/AB/f-GO/GCE sensors were able to detect 1 ag/mL of viral spike protein in synthetic, saliva, and oropharyngeal swab samples.

Fixed/screen-printed electrodes and the distinctive fingerprint of SARS-viral CoV-2's glycoproteins were used by Hashemi et al. [68] to develop a fast electrochemical biosensor. The working electrode of the sensor was activated by covering it with a layer of GO and sensitive chemical compounds (EDC: NHS), as well as gold nanostars. The sensor could detect viral traces in the aqueous biological medium, such as blood, by interacting with the active functional groups of the SARS-CoV-2 glycoproteins with a limit of detection of 1.68×10^{-22} µg/mL.

Using calixarene-functionalized GO, Zhao et al. [69] have developed an ultrasensitive electrochemical detection method for detecting SARS-CoV-2 RNA. The method was primarily based on a super sandwich-type recognition approach and was able to detect the RNA of SARS-CoV-2 using a portable electrochemical smartphone without the need for nucleic acid amplification and reverse transcription. The LOD for the clinical specimen was 200 copies per milliliter.

Sadique et al. [70] have created electrochemical immunosensor systems based on GO-Au nanocomposites for the simultaneous detection of SARS-CoV-2 antigens and antibodies. The features of the created GO-Au nanocomposites include strong conductivity, exceptional biocompatibility, and high surface functionality. The immunosensors were subjected to rigorous analysis using a redox electrolyte and synthetic samples, followed by validation using patient serum and nasopharyngeal swab samples to ensure accurate dual detection. Excellent sensitivity was exhibited by the SARS-CoV-2 antigen immunosensor with a LOD of 3.99 ag/mL, and the SARS-CoV-2 antibody immunosensor had a LOD of 1 fg/mL.

A specialized and highly responsive paper-based electrochemical immunosensor was created by Yakoh et al. [71] to detect immunoglobulins produced against SARS-CoV-2 (Figure 6). Through embedded GO, the working ePAD was used to immobilize spike protein RBD, which selectively binds to both IgG and IgM SARS-CoV-2 antibodies. The presence of SARS-CoV-2 antibodies interfered with the redox conversion of the redox indicator, leading to a reduction in the current. Clinical sera from actual patients were used to demonstrate the effectiveness of this electrochemical sensor, and the results showed a LOD of 1 ng/mL.

Electrochemical biosensors were created by Liv et al. [72] using EDC:NHS functionalized GO and modified glassy carbon electrodes in combination with wildtype and omicron SARS-CoV-2 nucleocapsid antibodies. These biosensors were able to detect the antigen in nasopharyngeal swab samples, and the lowest detection levels were 0.76 and 0.24 ag/mL for wildtype and omicron SARS-CoV-2 nucleocapsid antigen protein, respectively.

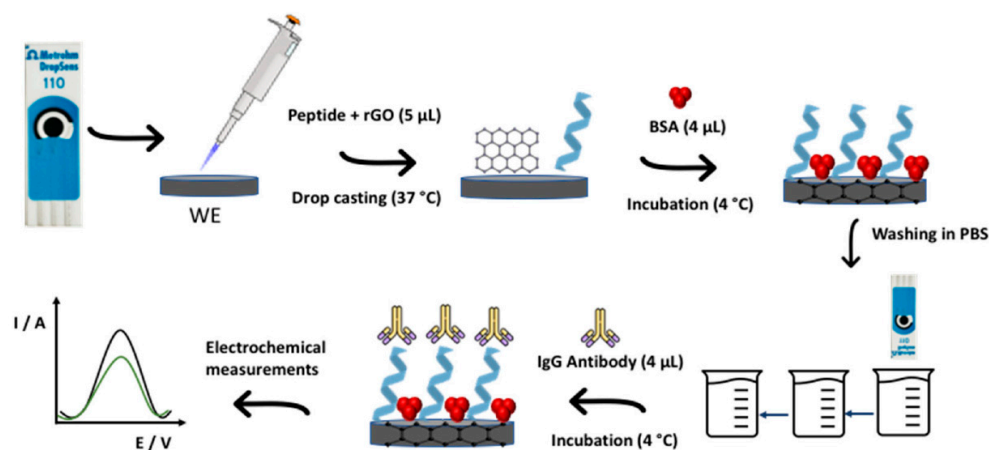


Figure 7. Schematic representation of immunosensor fabrication steps (Reprinted with permission from [74]).

2.1.4. Using Graphene Quantum Dots

A new method was devised by Martins et al. [75] for constructing immunosensors by attaching biological material to a screen-printed carbon electrode (SPE) that has been modified with electrodeposited Graphene Quantum Dots (GQD) and polyhydroxybutyric acid (PHB). The resultant electrode was employed as a functional substrate to recognize SARS-CoV-2 spike protein RBD to detect Anti-S antibodies with a LOD value of 100 ng/mL (Figure 8).

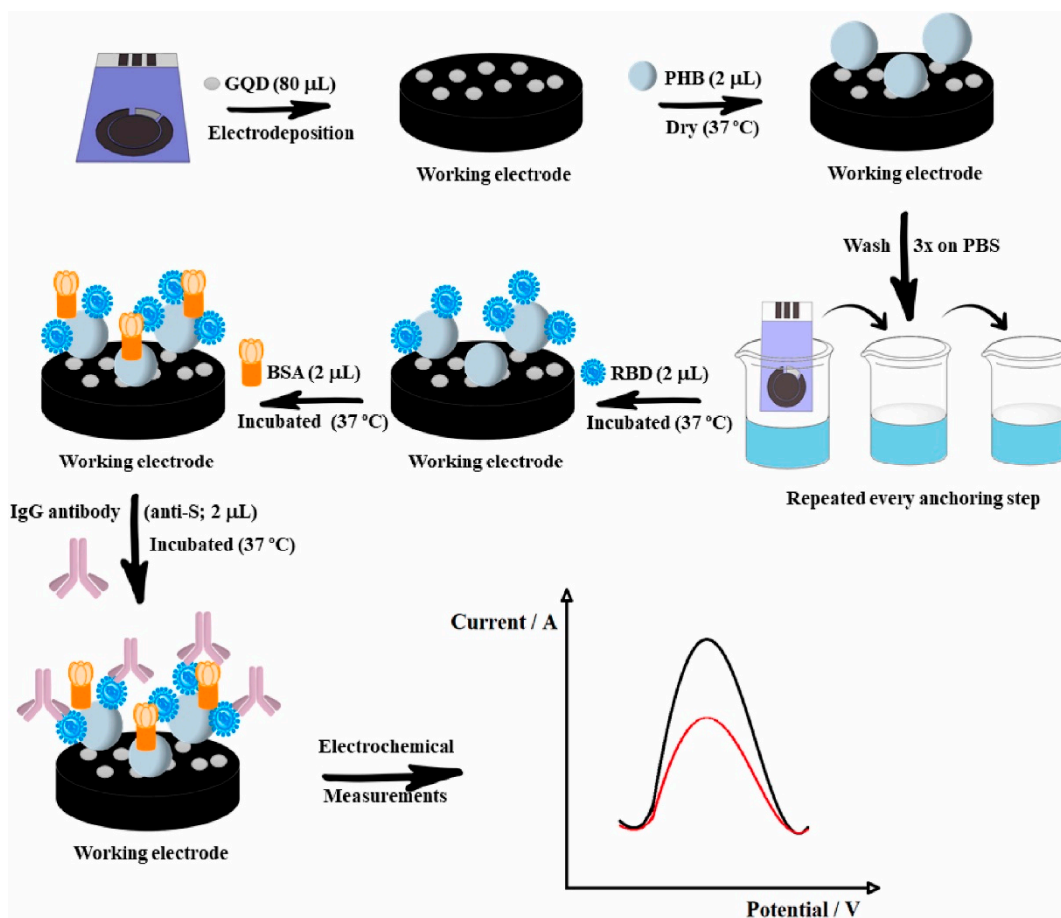


Figure 8. Immunosensor development stages (Reprinted with permission from [75]).

The prior discussion of Amperometric biosensors based on graphene for detecting SARS-CoV-2 is summarised in Table 3.

Table 3. Graphene-based Amperometric Biosensors for The Detection of SARS-CoV-2.

Key Carbon Material	Target	Limit of Detection (LOD)	Detection Range	Sensitivity	Response Time	Ref.
Graphene	Nucleocapsid protein, S1-IgG, S1-IgM and C-reactive protein	Nucleocapsid protein 0.1 µg/mL (serum) and 0.5 ng/mL (saliva) S1-IgG 2 µg/mL (serum) and 0.2 µg/mL (saliva) S1-IgM 20 µg/mL (serum) and 0.6 µg/mL (saliva) CRP 10 µg/mL (serum) and 0.1 µg/mL (saliva)	Nucleocapsid protein 0.1–0.8 µg/mL (serum) and 0.5–2.0 ng/mL (saliva) S1-IgG 2–40 µg/mL (serum) and 0.2–0.5 µg/mL (saliva) S1-IgM 20–50 µg/mL (serum) and 0.6–5.0 µg/mL (saliva) CRP 10–20 µg/mL (serum) and 0.1–0.5 µg/mL (saliva)	16.28 nA mL ng ⁻¹	1 min	Rodriguez et al. [54]
	Nucleocapsid Protein	2.0 fg/mL	0.1 pg/mL to 500 ng/mL	NA	120 min (incubation time)	Jaewjaroenwattana et al. [55]
	Nucleocapsid Antibody	13 fM	100 fM to 1 nM	NA	10 s	Ali et al. [56]
	Spike protein	2.9 ng/mL	2.9 to 500 ng/mL	NA	60 min (incubation time)	Beduk et al. [57]
	Spike protein	260 nM	NA	NA	45 min (incubation time)	Mojsoska et al. [58]
	Delta Variant (RNA)	1.2 pM	4 pM to 4 nM	NA	47 min	Yang et al. [59]
	RNA	100 fg/mL	100 fg/mL to 1 µg/mL	NA	30 min (hybridization time)	Damiati et al. [60]
	RNA	0.025 copies/µL	NA	NA	30 min for incubating, less than 1 min for detection	Ji et al. [61]
	cDNA	0.30 µmol/L	NA	0.583 µA µmol ⁻¹ L	30 min (hybridization time)	Silva et al. [62]
	RBD	0.8 ng/mL	2.5 to 40.0 ng/mL	NA	20 min (incubation time)	Tabrizi et al. [63]
RBD	0.36 ng/mL	0.5 to 250 ng/mL	NA	30 min	Tabrizi et al. [64]	
RBD	2 pg/mL	0.01 to 1500 ng/mL	NA	30 min (incubation time)	Primpray et al. [65]	
Graphene Oxide	Spike protein	0.58 pg/mL	1 pg/mL to 1 µg/mL	0.0105 mA/pg mL ⁻¹	NA	Kumar et al. [66]
	Spike Protein	1 ag/mL	1 ag/mL to 10 fg/mL	93.3% cm ⁻²	5 min	Liv et al. [67]
	Glycoprotein	1.68 × 10 ⁻²² µg/mL	NA	0.0048 µA µg ⁻¹ ·cm ⁻²	1 min	Hashemi et al. [68]
	RNA	200 copies/mL	NA	NA	NA	Zhao et al. [69]
	Nucleocapsid protein and immunoglobulin (Ig) G	Antigen (3.99 ag/mL) Antibody (1.0 fg/mL)	Antigen (10.0 ag/mL to 50.0 ng/mL) Antibody (1.0 fg/mL to 1.0 ng/mL)	NA	NA	Sadique et al. [70]
IgG and IgM	1 ng/mL	1 to 1000 ng/mL	100%	30 min (incubation time)	Yakoh et al. [71]	
Reduced Graphene Oxide Graphene Quantum Dots	Nucleocapsid protein	0.24 ag/mL	1 ag/mL to 10 fg/mL	NA	NA	Liv et al. [72]
	Spike protein	39.5 fmol/L	100 nmol/L to 500 fmol/L	NA	NA	El-Said et al. [73]
	Immunoglobulin G	0.77 µg/mL	NA	NA	60 min	Braz et al. [74]
	Anti-S antibodies (IgG)	100 ng/mL	100 ng/mL to 10 µg/mL	NA	120 min	Martins et al. [75]

2.2. Potentiometric Biosensors for the Detection of SARS-CoV-2

Biosensors based on the notion of electrochemical potential are called potentiometric biosensors. SARS-CoV-2 antigens or antibodies can be detected in a sample using potentiometric biosensors. The potential difference between the working and reference electrodes is measured by these biosensors [76]. Potentiometric biosensors contain viral protein-binding antibodies or antigens to detect SARS-CoV-2. Viral proteins attaching to the surface of antibodies or antigens cause a voltage shift at the working electrode in virus-containing samples. This potential shift allows qualitative or quantitative viral detection in the sample. Potentiometric biosensors can also be integrated with various transduction methods, such as FET (field-effect transistor) or solid-state electrodes, which are more robust and stable compared to traditional liquid-based electrodes [77].

2.2.1. Using Graphene

Hashemi et al. [78] developed an electrochemical diagnostic platform which was composed of activated GO and Au nanostars, for rapid and accurate detection of monoclonal IgG antibodies against the S1 protein of SARS-CoV-2 in blood samples from patients with COVID-19. The activated GO was made up of 8-hydroxyquinoline (8H) and 1-ethyl-3-(3-dimethylaminopropyl), as well as treated with EDC:NHS. The nanosensors were compre-

hensively characterized and successfully applied to enhance the performance of the glassy carbon electrode (GCE) and working electrode of DRP C110 carbon-based screen-printed electrode to detect the antibodies with a LOD of $0.18 \times 10^{-19}\%$ V/V.

To detect SARS-CoV-2, a FET-type sensor was developed by Li et al. [79] using MXene and graphene. The combination of MXene, a material with high chemical sensitivity, and graphene, a material with large-area and high-quality continuity, created an ultra-sensitive transduction material for sensing viruses. MXene–graphene surface was functionalized using (3-aminopropyl) triethoxysilane (APTES), which acted as a linker and allowed for the detection of viruses by taking advantage of the antibody–antigen interaction, resulting in electrochemical signal transduction (Figure 9). The FET sensor was integrated into a microfluidic channel, allowing it to detect viruses in solution directly, and exhibited a low limit of detection of 1 fg/mL for the recombinant 2019-nCoV spike protein.

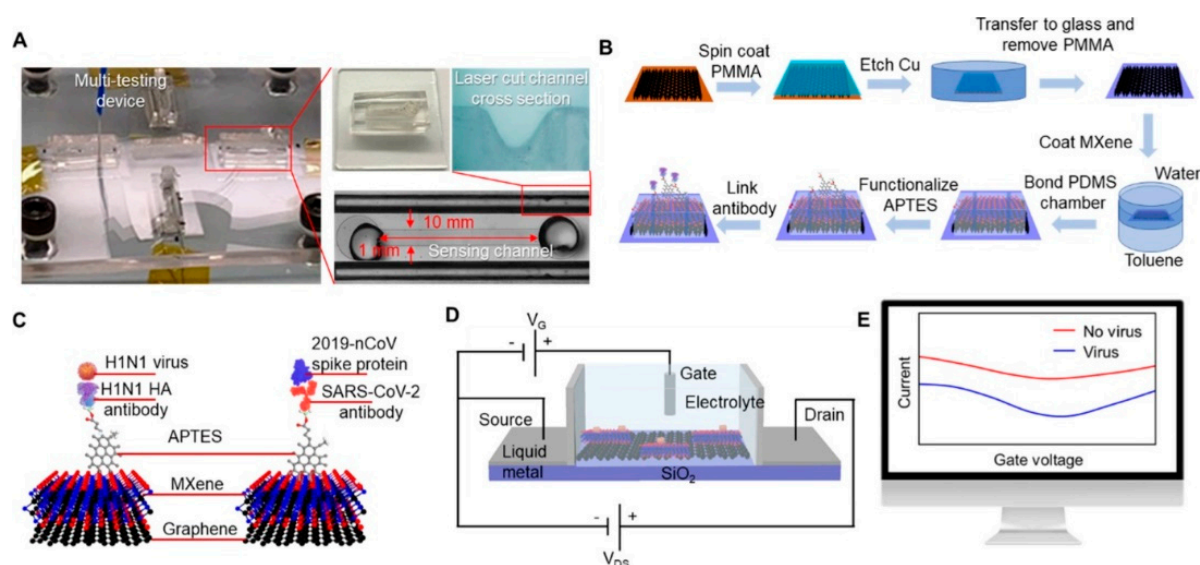


Figure 9. (A) Fabricated MXene-graphene field effect transistor sensor. (B) MXene-graphene virus-sensing transduction material deposition process, (C) Illustration of antibody-antigen sensing mechanism, (D) Field effect transistor circuit, and (E) Change in drain-source current. (Reprinted with permission from [79]).

Seo et al. [80] created a graphene field-effect transistor (GFET) engineered with an antibody specific to the SARS-CoV-2 spike protein. The SARS-CoV-2 spike antibody was bound with 1-pyrenebutanoic acid succinimidyl ester (PBASE), a probe linker. At a detection limit of 1 fg/mL, the GFET-based device was able to detect SARS-CoV-2 in both transport medium and clinical samples.

2.2.2. Using Graphene Oxide

To detect the SARS-CoV-2 nucleocapsid (N)-protein in a buffer, Novodchuk et al. [81] have investigated the potential of a transducer made of a boron and nitrogen co-doped graphene oxide gel (BN-GO gel) that was functionalized with nucleoprotein antibodies. The biosensor is based on a graphene field-effect transistor (FET) and demonstrates the ability to detect the viral protein in less than four minutes. The device exhibited an impressively low limit of detection of 10 ag/mL and a linear detection range spanning over 11 orders of magnitude, from 10 ag/mL up to 1 µg/mL (Figure 10).

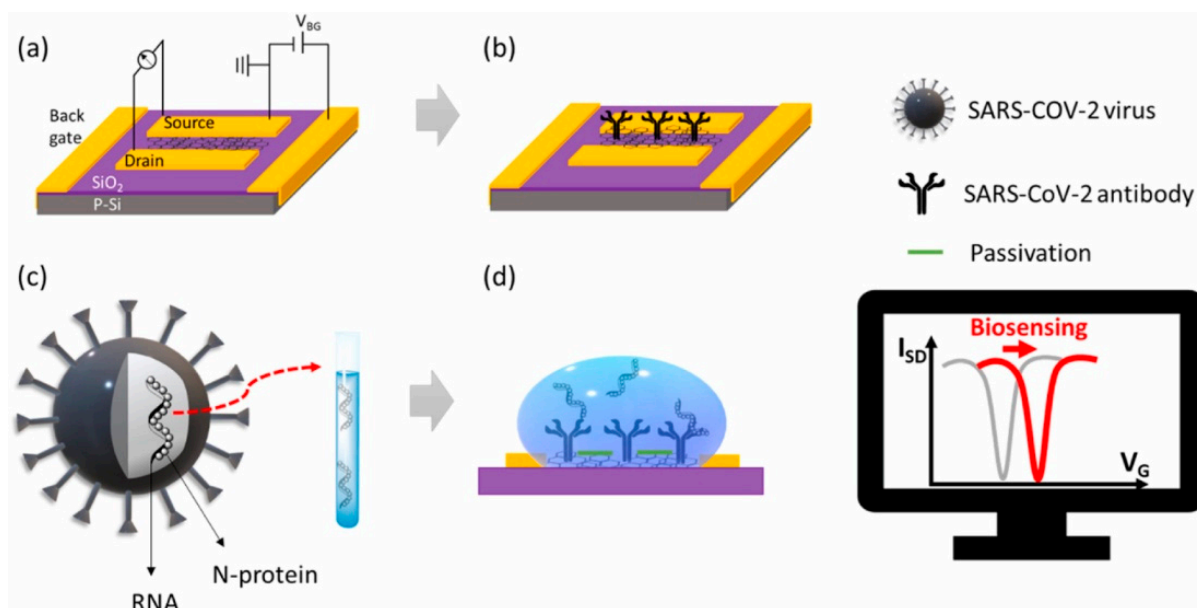


Figure 10. The device setup and biosensing process of the BN-GO gel FET SARS-CoV-2 N-protein biosensor is depicted using schematics. (a) The configuration of the back-gated FET device with the BN-GO gel channel positioned between the source and drain electrodes. (b) The configuration of the device following SARS-CoV-2 antibody functionalization and ethanolamine passivation. (c) In a buffer solution, the N-protein of the SARS-CoV-2 virus is diluted. (d) The biosensing response is defined by the voltage shift caused by the addition of the N-protein-containing solution. (Reprinted with permission from [81]).

Graphite oxide (GO-FET) field-effect transistors were integrated with COVID-19 antibodies by Wasfi et al. [82] to detect spike protein antigens in real-time. A graphite oxide channel between two gold electrodes was used to anchor magnetic spike antibodies specific to the COVID-19 spike protein to provide maximum selectivity and specificity. The GO-FET biosensor was further patterned with platinum-palladium bimetallic nanoparticles to increase sensitivity. The developed FET biosensor detected COVID-19 spike antigen at a LOD value of 1 fg/mL in phosphate-buffered saline.

2.2.3. Using Reduced Graphene Oxide

Krsihna et al. [83] created a silicon-based, label-free, reduced graphene oxide field-effect transistor (rGO FET) for detecting SARS-CoV-2. First, the APTES receptor was used to functionalize the rGO FET with SARS-CoV-2 monoclonal antibodies. Subsequently, the process of protein cross-linking and immobilization was carried out using EDC, hydrochloride, and Sulfo-NHS. Then, to test the antibody-antigen reaction of SARS-CoV-2 with different molar ranges, the distinctive response of the rGO FET was observed, which resulted in a detection limit of up to 0.002 fM.

Using graphene and gold nanoparticles, Li et al. [84] created a FET-type biosensing platform that could quickly and accurately detect SARS-CoV-2 RNAs from human throat swabs without any amplification steps (Figure 11). The sensor had special probes called complementary phosphorodiamidate morpholino oligos (PMOs), immobilized on the gold nanoparticle surface, that bind to SARS-CoV-2 RdRp, a key RNA molecule of the virus. The PMOs had no charges, which reduced noise and increased sensitivity. The platform was able to detect very low levels of SARS-CoV-2 RNAs in different samples with a low limit of detection, such as PBS (0.37 fM), throat swab (2.29 fM), and serum (3.99 fM).

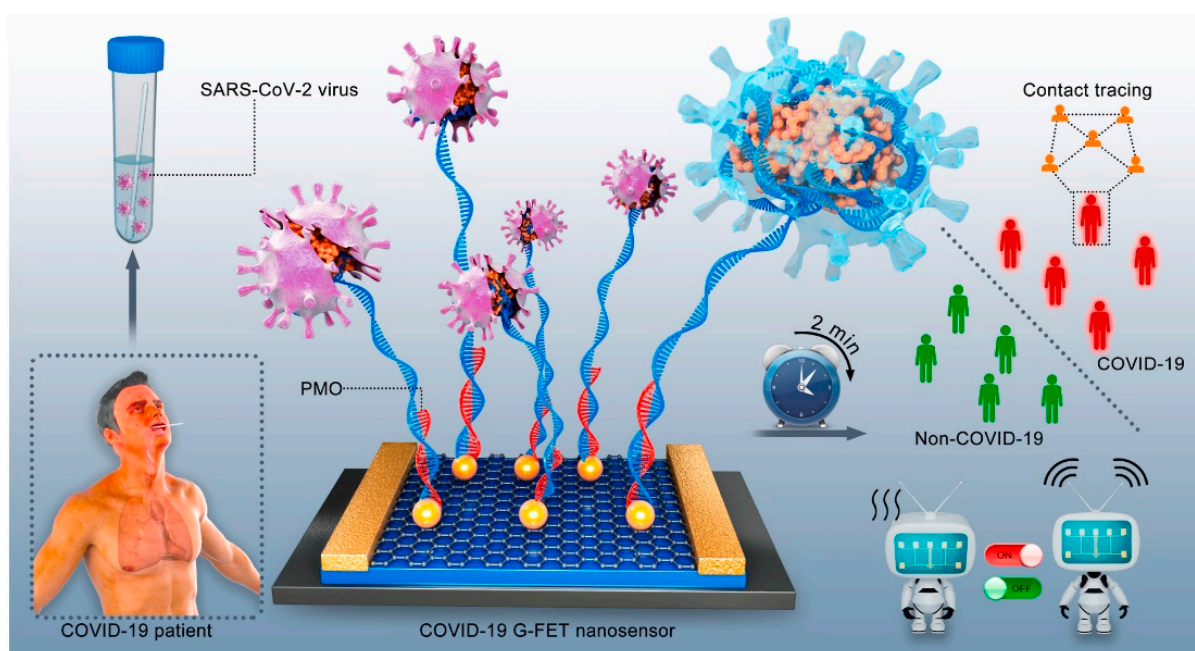


Figure 11. PCR-free quick, direct detection of COVID-19 utilizing the PMO-functionalized G-FET nanosensor is shown schematically. (Reprinted with permission from [84]).

To eliminate solution-interface instability and for standardization of 2D rGO sensing surfaces, Jang et al. [85] developed a remote floating-gate (RFG) FET configuration using rGO. Extensive tests of rGO-solution interfaces that varied in thickness, coverage, and reduction temperature were carried out to identify the key parameters that drive rGO's electrochemical instability. Finally, they showed that SARS-CoV-2 spike proteins could be reliably detected in saliva without the need for a label, with a detection limit of 3.4 pg/mL at concentrations ranging from 500 fg/mL to 5 g/mL.

The prior discussion of potentiometric biosensors based on graphene for detecting SARS-CoV-2 is summarised in Table 4.

Table 4. Graphene-based Potentiometric Biosensors for The Detection of SARS-CoV-2.

Key Carbon Material	Target	Limit of Detection (LOD)	Detection Range	Sensitivity	Response Time	Ref.
Graphene	IgG antibodies	$0.18 \times 10^{-19}\% V/V$	NA	$2.14 \mu A\% V/V \cdot cm^{-2}$	1 min	Hashemi et al. [78]
	Spike Protein	1 fg/mL	1 fg/mL to 10 pg/mL	NA	50 ms	Li et al. [79]
	Spike protein	1 fg/mL	NA	NA	1 min	Seo et al. [80]
Graphene oxide	Nucleocapsid protein	10 ag/mL	10 ag/mL to 1 μ g/mL	NA	4 min	Novodchuk et al. [81]
	Spike protein	1 fg/mL	1 fg/mL to 100 ng/mL)	NA	NA	Wasfi et al. [82]
Reduced graphene oxide	Spike protein	0.002 fM	NA	NA	NA	Krsihna et al. [83]
	RNA	PBS (0.37 fM), throat swab (2.29 fM), and serum (3.99 fM)	NA	NA	2 min	Li et al. [84]
	Spike protein	3.4 pg/mL	500 fg/mL to 5 μ g/mL	5.1 mV/dec	NA	Jang et al. [85]

2.3. Impedimetric Biosensors for the Detection of SARS-CoV-2

To detect target analytes, impedimetric biosensors apply the principle of electrical impedance. Samples containing SARS-CoV-2 antigens or antibodies can be detected using impedimetric biosensors. An electrical impedance measurement is taken across the working electrode of these biosensors [86]. SARS-CoV-2 attaches to surface antibodies or antigens, changing the biosensor's working electrode's electrical impedance. This impedance shift can detect viruses qualitatively or quantitatively. Impedimetric biosensors offer the advantage of high sensitivity and specificity and can be integrated with various transduction methods such as Quartz Crystal Microbalance (QCM), Interdigitated Array (IDA), or Elec-

trochemical Impedance Spectroscopy (EIS) to enhance the sensitivity and specificity of the biosensors [87,88].

2.3.1. Using Graphene

A 3D-printed COVID-19 immunosensor was developed by Muñoz et al. [89] using a bottom-up biofunctionalization approach by covalently attaching a COVID-19 recombinant protein to a 3D-printed graphene-based nanocomposite electrode surface. The electrode was first functionalized with Au-NPs using an inner-matrix synthesis approach. Then, it was treated with cysteamine and glutaraldehyde solutions to covalently link COVID-19 recombinant protein as the recognition biomarker to the electrode's amine groups via terminal aldehyde groups on the linker. The sensor used electrical impedance to detect changes at the electrode/electrolyte interface when interacting with a monoclonal COVID-19 antibody. The system depicted a low detection limit of $0.5 \pm 0.1 \mu\text{g/mL}$ and has been shown to work well in both buffered and human serum samples.

Ehsan et al. [90] developed a biosensor for the detection of the SARS-CoV-2 spike protein that utilized an IgG anti-SARS-CoV-2 spike antibody. The biosensor employed SPEs that obey the principle of redox reaction impedance to probe antigen spikes. The biosensor used high conductivity graphene/carbon ink to achieve a small background impedance leading to a wide dynamic range of detection. The antibody is immobilized onto the electrode surface through either a chemical (1-pyrenebutanoic acid succinimidyl ester) or biological entity (staphylococcal protein A), with the latter method resulting in enhanced sensitivity and a very low limit of detection of 0.25 fg/mL .

A quick and facile method for detecting SARS-CoV-2 antibodies was developed by Ali et al. [91] using a 3D biosensing platform made from nanomaterials. The platform features an array of micropillar electrodes created using 3D printing and aerosolized gold nanoparticles and coated with graphene nanoflakes and certain SARS-CoV-2 antigens (Figure 12). The sensor surfaces were used to immobilize the S1, RBD, and N antigens individually, which served as the capturing elements for the corresponding antibodies present in human plasma samples from patients infected with SARS-CoV-2. The sensor operated on electrochemical transduction, where viral proteins on the sensor electrode surface interacted with antibodies to change sensor impedance with a LOD of 10 fM .

Alafeef et al. [92] created a rapid, inexpensive, easy-to-use paper-based electrochemical biosensor to detect SARS-CoV-2 digitally. Gold nanoparticles with specific antisense oligonucleotides were used to detect nucleocapsid phosphoproteins. Finally, a nucleic-acid-testing device with a hand-held reader was created by immobilizing sensing probes (ssDNA-capped gold nanoparticles) on a paper-based substrate. Clinical and SARS-CoV-2-infected Vero cell samples were evaluated using the biosensor chip. The sensor has a sensitivity of $231 (\text{copies } \mu\text{L}^{-1})^{-1}$ and a limit of detection of $6.9 \text{ copies}/\mu\text{L}$ without amplification.

To develop a fast electrochemical immunosensor for rapid identification of SARS-CoV-2 spike RBD in saliva samples, Pola et al. [93] used custom-made graphene inks in combination with aerosol jet printing. The rapid response time (30 min) and low detection limits ($22.91 \pm 4.72 \text{ pg/mL}$) of this sensor might be attributed to the single-step functionalization of printed graphene electrodes with SARS-CoV-2 polyclonal antibody via the carbodiimide reaction (EDC:NHS).

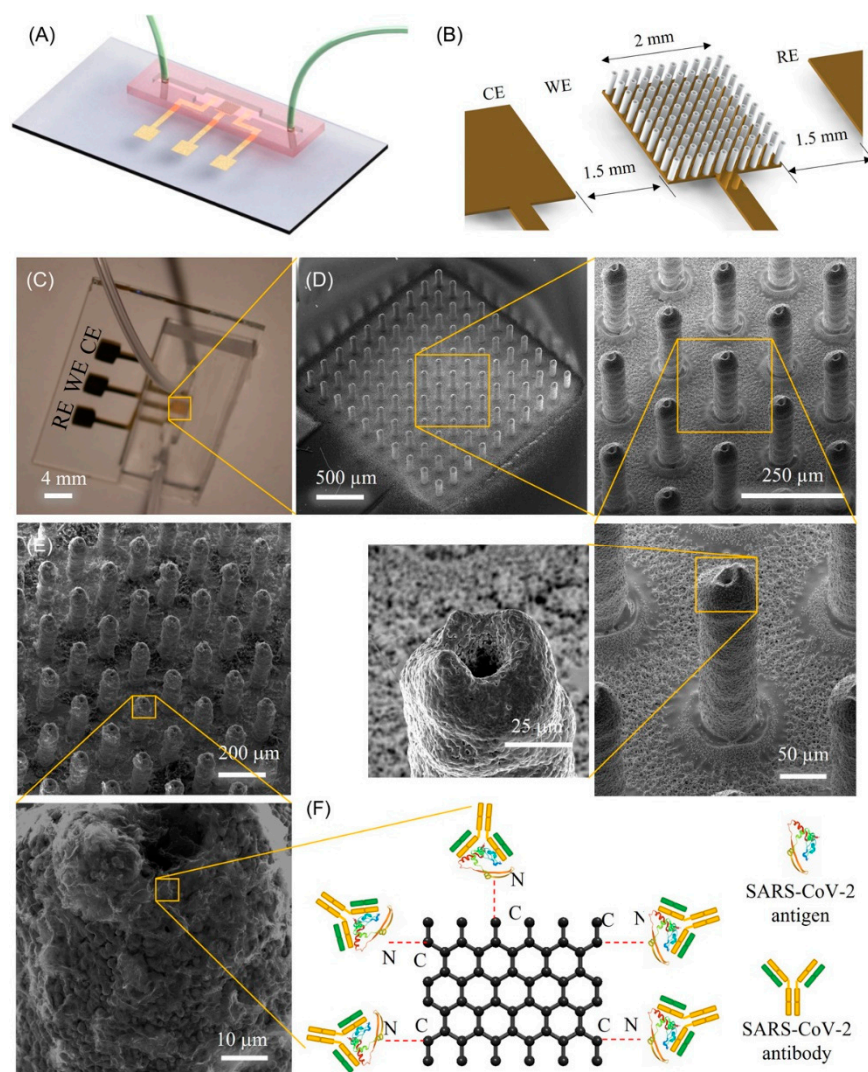


Figure 12. A biosensor designed for in vitro detection of SARS-CoV-2 antibodies in patients with COVID-19 has been fabricated using 3D printing technology. (A,B) The figures depict a 3D-printed microfluidic sensor in which the working electrode (WE) is composed of an array of gold nanoparticles arranged in micropillars. The working electrode is located between the reference electrode (RE) and the counter electrode (CE). (C) An optical photograph of a real device. (D) Scanning electron microscope (SEM) images of the printed micropillar array were captured from various angles and magnifications before the application of graphene and proteins. The SEM images show the microtexture of the sintered gold micropillars at high magnification, which facilitates the attachment of reduced graphene oxide (rGO) nanoflakes to the surface. (E) A scanning electron microscope (SEM) image depicting the array electrode with reduced graphene oxide (rGO) nanoflakes applied to the surface. (F) This schematic illustration demonstrates the functionalization process of attaching SARS-CoV-2 proteins onto reduced graphene oxide (rGO) sheets using EDC: NHS conjugation chemistry. During the amidation reaction, EDC activates the COOH groups of rGO, and NHS acts as a stabilizer to form amide bonds between the proteins and rGO sheets on the surface of the gold pillar. Additionally, the diagram depicts antibodies that attach to the SARS-CoV-2 proteins during sensing. (Reprinted with permission from [91]).

2.3.2. Using Graphene Oxide

Graphene oxide nanocolloids (GONC) were used by Ang et al. [94] as a transducing platform and also an electroactive label for the detection of 2019-nCoV genomic sequences. GONC is an easy-to-use and very sensitive biosensing platform due to the intrinsic electrochemical signal resulting from the reduction of the electrochemically reducible oxygen

functions that exist on the surface. After immobilizing a single-stranded DNA probe and incubating it with varying concentrations of the target 2019-nCoV DNA strand, the intrinsic electroactivity of the material was measured at each stage of the genosensing procedure to achieve a LOD of 186×10^{-9} M (Figure 13).

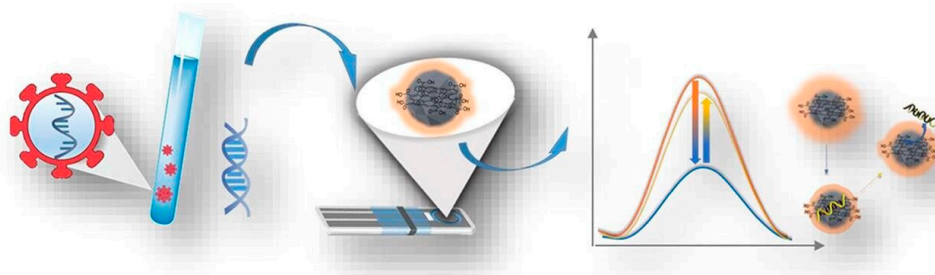


Figure 13. (Left) Incubation of SARS-CoV-2 ssDNA with cDNA-modified GONC on a miniaturized disposable chip. (Right) GONC signal restoration in the presence of viral DNA. (Reprinted with permission from [94]).

2.3.3. Using Reduced Graphene Oxide

Ali et al. [95] reported that COVID-19 antibodies could be detected in seconds using a novel nanomaterial-based biosensing technology. Nanoprinting of 3D gold electrodes, covering the electrodes with rGO nanoflakes, and immobilization of certain viral antigens (spike S1 and RBD) on the rGO nanoflakes using an EDC:NHS chemistry contributed to the creation of the biosensing platform (Figure 14). After being combined with a microfluidic device, the electrode was employed in a regular electrochemical cell. Impedance spectroscopy was used to detect changes in the electrical circuit caused by the binding of antibodies to antigens on the electrode with LOD values of 2.8×10^{-15} M (S1) and 16.9×10^{-15} M (RBD), and the results could be viewed with a smartphone app.

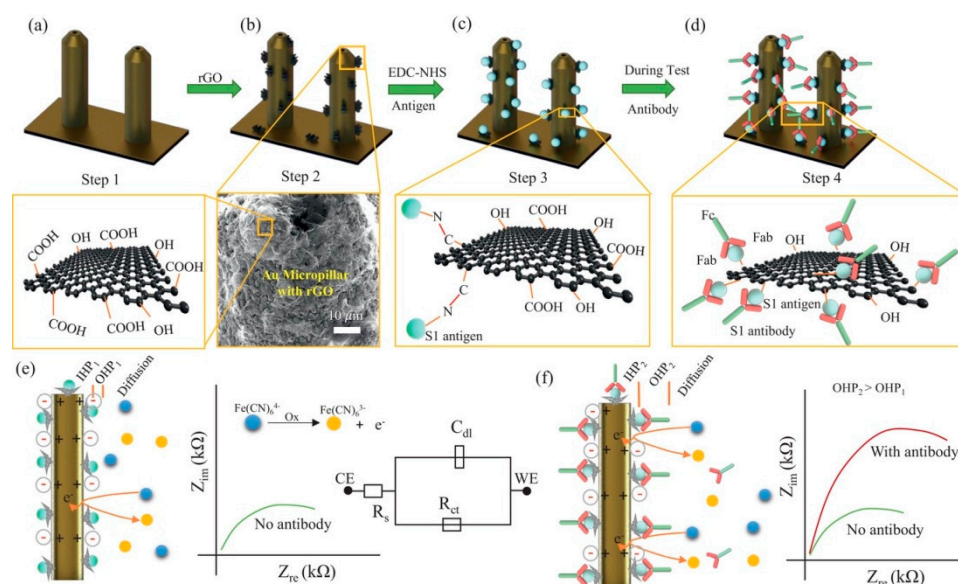


Figure 14. 3D-printed micropillar electrode functionalization and operation of 3DcC sensor. (a) Aerosol Jet printed gold micropillars before surface treatment (step 1) (b) A straightforward drop-casting technique is utilized to coat the electrodes with carboxylated rGO sheets (step 2) (c) Attaching the proteins from the virus to the rGO layers using a chemical reaction with EDC: NHS (step 3) (d) Antibodies only stuck to the matching antigens when they came into contact with the sensor (step 4) (e,f) Schematics showing the sensing principle of the 3DcC device. (Reprinted with permission from [95]).

Zaccariotto et al. [96] explored the benefits of antibody immobilization on rGO to devise a new impedimetric immunosensor-based technique for detecting SARS-CoV-2. Activated recombinant human coronavirus SARS-CoV-2, Spike Glycoprotein RBD was immobilized on the rGO surface employing EDC:NHS chemistry. The impedimetric immunosensor and a redox couple were used as probes in an electrochemical immunoassay for the identification of SARS-CoV-2 spike protein RBD with a LOD of 150 ng/mL.

Haghighyegh et al. [97] used an electrochemical method for detecting SARS-CoV-2 nucleocapsid protein antigens that relied on carbon SPEs with a coating of a highly stable buffer-based ZnO/rGO nanocomposite. Nanomaterial creation on the electrode surface is streamlined to a single step by utilizing a salt-based (ionic) matrix for homogeneous dispersion of the nanocomposite. With a linear range of 1–10,000 pg/mL, the immunobiosensor had a detection limit of 21 fg/mL.

The prior discussion of Impedimetric biosensors based on graphene for detecting SARS-CoV-2 is summarised in Table 5.

Table 5. Graphene-based Impedimetric Biosensors for The Detection of SARS-CoV-2.

Key Carbon Material	Target	Limit of Detection (LOD)	Detection Range	Sensitivity	Response Time	Ref.
Graphene	Spike Protein	0.5 ± 0.1 µg/mL	1.0 to 10 µg/mL	0.076 ppm ⁻¹	20 min	Muñoz et al. [89]
	Spike Protein Nucleocapsid (N), spike 1 (S1), and RBD proteins	0.25 fg/mL	0.25 fg/mL to 1 µg/mL	NA	5 min	Ehsan et al. [90]
	Nucleocapsid phosphoprotein (N-gene)	1 pm (N), 0.1 pm (S1), 10 fM (RBD)	10 fM to 50 nM	100%	10–12 s	Ali et al. [91]
Graphene Oxide	Spike RBD Gene	6.9 copies/µL	585.4 to 5.854 × 10 ⁷ copies/µL	231 (copies µL ⁻¹) ⁻¹	5 min	Alafeef et al. [92]
	Spike RBD Gene	22.91 ± 4.72 pg/mL	1 to 1000 ng/mL	NA	30 min	Pola et al. [93]
	Spike RBD Gene	186 × 10 ⁻⁹ M	10 ⁻¹⁰ to 10 ⁻⁵ M	NA	NA	Ang et al. [94]
Reduced Graphene Oxide	Spike (S1) and RBD proteins	2.8 × 10 ⁻¹⁵ M (S1) 16.9 × 10 ⁻¹⁵ M (RBD)	NA	1 × 10 ⁻¹² M (S1) 1 × 10 ⁻¹⁵ M (RBD)	12 s	Ali et al. [95]
	spike protein RBD	150 ng/mL	0.16 to 40 µg/mL	NA	NA	Zaccariotto et al. [96]
	nucleocapsid (N-) protein antigens	21 fg/mL	1 to 10,000 pg/mL	32.07 ohms·mL/pg·mm ²	15 min	Haghighyegh et al. [97]

3. Current Challenges and Future Perspectives

The development of graphene-based electrochemical biosensors for the detection of SARS-CoV-2 and other analytes is an active area of research. While graphene-based biosensors have many advantages, such as high sensitivity, selectivity, and fast response times, there are also several challenges that need to be overcome to make them practical for use in real-world applications.

The use of graphene in practical applications is still limited due to the lack of chemical reactivity and solubility in most solvents. Therefore, one of the significant challenges in the field of graphene research is to functionalize graphene by adding chemical groups to its surface to modify its properties, improve its solubility, and create new structures. Functionalization of graphene, however, poses some significant challenges. One such challenge is maintaining the structural integrity of graphene. The process of functionalization may introduce defects or damage to its structure, which can adversely affect its properties [98]. Another hurdle is controlling the degree and location of functionalization, as these can significantly affect the properties of graphene [99]. As different applications may require different functionalization strategies, it is necessary to develop versatile and efficient functionalization methods that can be tailored to meet the specific requirements of different applications and yield high-quality, reproducible products in large quantities. Functionalized graphene must be stable and durable under various conditions to ensure its long-term performance in practical applications, which is another major obstacle in graphene functionalization.

The potential toxicity of graphene is a concern that has been extensively studied in recent years [100]. While graphene itself is considered to be biocompatible and non-toxic, there are concerns about the toxicity of graphene-based materials (GBMs), which are composites that contain graphene or graphene oxide [101]. Studies have shown that

the toxicity of GBMs depends on a variety of factors, such as size, shape, concentration, and surface functionalization [102]. In general, GBMs that are smaller in size and have a higher surface area-to-volume ratio tend to be more toxic than larger GBMs [103]. The toxicity of GBMs can also be influenced by their shape, with more elongated particles being more toxic than spherical particles [104]. Another factor that can affect the toxicity of GBMs is their concentration. At high concentrations, GBMs can induce cell death and inflammation, which can be harmful to living organisms [105]. Furthermore, the surface functionalization of GBMs can also impact their toxicity. Certain surface functional groups, such as carboxyl and amino groups, can reduce the toxicity of GBMs by increasing their biocompatibility [102]. Notwithstanding legitimate concerns about GBM toxicity, it is worth noting that many of the studies have employed GBM concentrations well above those generally encountered in practice. [106]. Moreover, the potentially toxic effects of GBMs can be mitigated by using appropriate safety measures and developing methods to minimize their release into the environment [107] or using green methods for the entire process [108,109].

Another challenge is the integration of graphene-based biosensors with microfluidic devices for sample preparation and manipulation [110]. This can be difficult due to the handling and integration of the graphene material and the need for precise control of the fluidic flow and manipulation [111]. The integration and miniaturization of sensors can be impeded by solution-gated sensors [80] as they usually necessitate an external electrode that must be inserted into the electrolyte solution. Biological samples can be complex, containing a wide range of molecules, which can interfere with the detection of the analyte of interest [112]. The amount of sample available for analysis is generally limited, which can affect the sensitivity and accuracy of the biosensor. Biological samples mostly have stability issues, which are affected by factors such as temperature, pH, and time. This can potentially impact the reproducibility of the biosensor measurements [113]. Non-specific binding of other molecules in the sample to the biosensor surface leads to false-positive signals, reducing the specificity of the biosensor. The sample preparation protocol should be compatible with the biosensor surface and should not damage or alter it, as this can affect the sensitivity and accuracy of the biosensor. The efficient extraction and purification of viral RNA from patient samples are also crucial for accurate detection but are still a major challenge [114].

Limitations in the scalability and cost-effectiveness of graphene biosensors may arise from the high cost of generating high-quality graphene. Graphene's production cost can be lowered by upgrading production methods and exploring novel synthetic processes [115,116]. Graphene biosensors are costly and difficult to mass produce due to their complex fabrication process. This problem can be solved by streamlining the production procedure, enhancing the efficiency of existing production methods, and introducing more automated processes [117].

The quality of graphene may vary depending on the production method and conditions [118], which can lead to variations in the performance of graphene biosensors. The surface functionalization of graphene can also vary, affecting the specificity and sensitivity of graphene biosensors. Variations in device fabrication, such as variations in the thickness and quality of dielectric layers, may affect the performance of graphene biosensors [119]. Variations in measurement conditions, such as temperature, humidity, and buffer solutions, can affect the performance of graphene biosensors. It was reported that graphene-based sensors' resistance changes when they come into contact with liquids that include free fluorescein [120].

Another challenge is the lack of standardization in the fabrication and characterization of graphene-based biosensors. The lack of standardization in commercially available graphene due to differences in production methods hinders its commercialization [121]. The absence of standardized manufacturing processes and characterization techniques is also a major challenge in the development and commercialization of graphene biosensors. Variations in manufacturing methods and conditions can significantly affect the quality

and performance of graphene biosensors. Similarly, differences in the characterization technique can lead to discrepancies in the reported performance of graphene biosensors [122]. This makes it difficult to compare results from different research groups and to develop a consensus on the best ways to use these sensors. Moreover, there is a lack of collaboration and coordination between research groups and industry, which hinders the development of standardized protocols for graphene biosensors. This highlights the need for concerted efforts to establish uniform and consistent procedures for the manufacturing, characterization, and testing graphene biosensors. By doing so, it will be possible to achieve reproducible and reliable results that are essential for the advancement of graphene biosensors toward widespread adoption in clinical and commercial settings.

The miniaturization and rapid screening for SARS-CoV-2 using graphene-based sensors also present several obstacles. One of the primary hurdles is achieving high sensitivity and specificity to accurately detect the virus, which requires careful selection of graphene material and optimization of sensor design and fabrication processes. Another obstacle is developing a robust and reliable biosensing platform capable of handling a large number of samples simultaneously for high-throughput screening [123]. Additionally, creating a portable and low-cost device for on-site testing poses a challenge [124]. The device must be user-friendly, with a long shelf-life and stability under various environmental conditions. Finally, obtaining regulatory approval for the use of graphene-based biosensors in clinical settings is a significant hurdle [125]. The sensors must undergo rigorous testing and validation to ensure their safety and efficacy before receiving widespread approval.

To date, several SARS-CoV-2 test kits utilizing oropharyngeal swabs, nasopharyngeal swabs, or oral saliva as a sample have been introduced in the market [126,127]. Recent studies have indicated that the use of saliva samples for COVID-19 testing offers numerous advantages over swabs, such as increased patient comfort, ease of collection, reduced exposure risk, and comparable or superior accuracy [128–131]. Consequently, researchers are increasingly interested in developing saliva-based test kits for SARS-CoV-2 [132,133]. Despite the numerous benefits of rapid antigen tests, commercially available COVID-19 test kits are associated with several drawbacks, including false negative results, limited accuracy, variability in test quality, and, most importantly, lack of standardization [134–139]. Although COVID-19 test kits have been instrumental in controlling the spread of the virus, their use is limited by these drawbacks and limitations [140]. Therefore, it is essential to continue improving the accuracy, availability, and affordability of these tests to manage the pandemic better.

4. Conclusions

In conclusion, the use of graphene-based electrochemical biosensors for the detection of SARS-CoV-2 is a promising area of research. The various types of graphene-based electrochemical biosensors, including amperometric, potentiometric, and impedimetric biosensors, have been reviewed, and the current challenges associated with their use have been discussed. While graphene-based electrochemical biosensors have many advantages, such as high sensitivity, selectivity, and fast response times, there are also several challenges that need to be overcome to make them practical for use in real-world applications. These challenges include the functionalization of graphene, potential toxicity of graphene, integration with microfluidic devices, effective sample preparation, upscaling, reproducibility, and, finally, standardization. Despite these challenges, there is a lot of potential for graphene-based electrochemical biosensors in the detection of SARS-CoV-2 and other analytes. Future research in this field will focus on developing more efficient and robust functionalization methods, as well as on the integration of graphene-based biosensors with microfluidic devices and other detection technologies to improve the sensitivity, selectivity, and practicality of these biosensors. Additionally, the development of cost-effective production methods for graphene materials is also crucial to make these biosensors more accessible and commercially viable. Overcoming these challenges will require further research and development, but the potential benefits of using graphene-based biosensors

for the detection of SARS-CoV-2 make this a worthwhile pursuit. The use of such sensors may aid in the early detection and control of future pandemics.

Author Contributions: Conceptualization, C.M.H.; methodology, J.S.; writing—original draft preparation, J.S.; writing—review and editing, C.M.H. All authors have read and agreed to the published version of the manuscript.

Funding: This research received no external funding.

Conflicts of Interest: The authors declare no conflict of interest.

References

1. Jayaweera, M.; Perera, H.; Gunawardana, B.; Manatunge, J. Transmission of COVID-19 Virus by Droplets and Aerosols: A Critical Review on the Unresolved Dichotomy. *Environ. Res.* **2020**, *188*, 109819. [CrossRef]
2. Karia, R.; Gupta, I.; Khandait, H.; Yadav, A.; Yadav, A. COVID-19 and Its Modes of Transmission. *SN Compr. Clin. Med.* **2020**, *2*, 1798–1801. [CrossRef] [PubMed]
3. Lauer, S.A.; Grantz, K.H.; Bi, Q.; Jones, F.K.; Zheng, Q.; Meredith, H.R.; Azman, A.S.; Reich, N.G.; Lessler, J. The Incubation Period of Coronavirus Disease 2019 (COVID-19) from Publicly Reported Confirmed Cases: Estimation and Application. *Ann. Intern. Med.* **2020**, *172*, 577–582. [CrossRef] [PubMed]
4. Li, X.; Zhong, X.; Wang, Y.; Zeng, X.; Luo, T.; Liu, Q. Clinical Determinants of the Severity of COVID-19: A Systematic Review and Meta-Analysis. *PLoS ONE* **2021**, *16*, e0250602. [CrossRef] [PubMed]
5. WHO. Coronavirus (COVID-19) Dashboard. Available online: <https://covid19.who.int> (accessed on 17 March 2023).
6. Carabelli, A.M.; Peacock, T.P.; Thorne, L.G.; Harvey, W.T.; Hughes, J.; de Silva, T.I.; Peacock, S.J.; Barclay, W.S.; de Silva, T.I.; Towers, G.J.; et al. SARS-CoV-2 Variant Biology: Immune Escape, Transmission and Fitness. *Nat. Rev. Microbiol.* **2023**, *21*, 162–177. [CrossRef]
7. Wei, X.; Li, L.; Zhang, F. The Impact of the COVID-19 Pandemic on Socio-Economic and Sustainability. *Environ. Sci. Pollut. Res.* **2021**, *28*, 68251–68260. [CrossRef]
8. Centers for Disease Control and Prevention. *COVID Data Tracker*; US Department of Health and Human Services, CDC: Atlanta, GA, USA, 2022. Available online: <https://covid.cdc.gov/covid-data-tracker> (accessed on 11 April 2023).
9. Wang, C.; Liu, Z.; Chen, Z.; Huang, X.; Xu, M.; He, T.; Zhang, Z. The Establishment of Reference Sequence for SARS-CoV-2 and Variation Analysis. *J. Med. Virol.* **2020**, *92*, 667–674. [CrossRef]
10. Pizzato, M.; Baraldi, C.; Boscato Sopetto, G.; Finozzi, D.; Gentile, C.; Gentile, M.D.; Marconi, R.; Paladino, D.; Raoss, A.; Riedmiller, I.; et al. SARS-CoV-2 and the Host Cell: A Tale of Interactions. *Front. Virol.* **2022**, *1*, 815388. [CrossRef]
11. Santos, I.d.A.; Grosche, V.R.; Bergamini, F.R.G.; Sabino-Silva, R.; Jardim, A.C.G. Antivirals Against Coronaviruses: Candidate Drugs for SARS-CoV-2 Treatment? *Front. Microbiol.* **2020**, *11*, 1818. [CrossRef]
12. Rahman, M.M. Progress in Electrochemical Biosensing of SARS-CoV-2 Virus for COVID-19 Management. *Chemosensors* **2022**, *10*, 287. [CrossRef]
13. Cassidy, A.; Parle-McDermott, A.; O’Kennedy, R. Virus Detection: A Review of the Current and Emerging Molecular and Immunological Methods. *Front. Mol. Biosci.* **2021**, *8*, 637559. [CrossRef] [PubMed]
14. Sengupta, J.; Hussain, C.M. The Emergence of Carbon Nanomaterials as Effective Nano-Avenues to Fight against COVID-19. *Materials* **2023**, *16*, 1068. [CrossRef]
15. Murillo, A.M.M.; Tomé-Amat, J.; Ramírez, Y.; Garrido-Arandia, M.; Valle, L.G.; Hernández-Ramírez, G.; Tramarin, L.; Herreros, P.; Santamaría, B.; Díaz-Perales, A.; et al. Developing an Optical Interferometric Detection Method Based Biosensor for Detecting Specific SARS-CoV-2 Immunoglobulins in Serum and Saliva, and Their Corresponding ELISA Correlation. *Sens. Actuators B Chem.* **2021**, *345*, 130394. [CrossRef]
16. Kaushik, A.K.; Dhau, J.S.; Gohel, H.; Mishra, Y.K.; Kateb, B.; Kim, N.-Y.; Goswami, D.Y. Electrochemical SARS-CoV-2 Sensing at Point-of-Care and Artificial Intelligence for Intelligent COVID-19 Management. *ACS Appl. Bio Mater.* **2020**, *3*, 7306–7325. [CrossRef] [PubMed]
17. Mandal, D.; Indaleeb, M.M.; Younan, A.; Banerjee, S. Piezoelectric Point-of-Care Biosensor for the Detection of SARS-COV-2 (COVID-19) Antibodies. *Sens. Bio Sens. Res.* **2022**, *37*, 100510. [CrossRef]
18. Zhang, J.Z.; Yeh, H.-W.; Walls, A.C.; Wicky, B.I.M.; Sprouse, K.R.; VanBlargan, L.A.; Treger, R.; Quijano-Rubio, A.; Pham, M.N.; Kraft, J.C.; et al. Thermodynamically Coupled Biosensors for Detecting Neutralizing Antibodies against SARS-CoV-2 Variants. *Nat. Biotechnol.* **2022**, *40*, 1336–1340. [CrossRef] [PubMed]
19. Wu, K.; Saha, R.; Su, D.; Krishna, V.D.; Liu, J.; Cheeran, M.C.-J.; Wang, J.-P. Magnetic-Nanosensor-Based Virus and Pathogen Detection Strategies before and during COVID-19. *ACS Appl. Nano Mater.* **2020**, *3*, 9560–9580. [CrossRef]
20. Guliy, O.; Zaitsev, B.; Teplykh, A.; Balashov, S.; Fomin, A.; Staroverov, S.; Borodina, I. Acoustical Slot Mode Sensor for the Rapid Coronavirus Detection. *Sensors* **2021**, *21*, 1822. [CrossRef] [PubMed]
21. Drobys, M.; Ramanaviciene, A.; Viter, R.; Chen, C.-F.; Samukaite-Bubniene, U.; Ratautaite, V.; Ramanavicius, A. Biosensors for the Determination of SARS-CoV-2 Virus and Diagnosis of COVID-19 Infection. *Int. J. Mol. Sci.* **2022**, *23*, 666. [CrossRef]

22. Chaibun, T.; Puenpa, J.; Ngamdee, T.; Boonapatcharoen, N.; Athamanolap, P.; O'Mullane, A.P.; Vongpunsawad, S.; Poovorawan, Y.; Lee, S.Y.; Lertanantawong, B. Rapid Electrochemical Detection of Coronavirus SARS-CoV-2. *Nat. Commun.* **2021**, *12*, 802. [[CrossRef](#)]
23. Rasmi, Y.; Li, X.; Khan, J.; Ozer, T.; Choi, J.R. Emerging Point-of-Care Biosensors for Rapid Diagnosis of COVID-19: Current Progress, Challenges, and Future Prospects. *Anal. Bioanal. Chem.* **2021**, *413*, 4137–4159. [[CrossRef](#)] [[PubMed](#)]
24. Sengupta, J.; Hussain, C.M. Decadal Journey of CNT-Based Analytical Biosensing Platforms in the Detection of Human Viruses. *Nanomaterials* **2022**, *12*, 4132. [[CrossRef](#)] [[PubMed](#)]
25. Sengupta, J.; Hussain, C.M. Graphene and Its Derivatives for Analytical Lab on Chip Platforms. *TrAC Trends Anal. Chem.* **2019**, *114*, 326–337. [[CrossRef](#)]
26. Kamedulski, P.; Skorupska, M.; Binkowski, P.; Arendarska, W.; Ilnicka, A.; Lukaszewicz, J.P. High Surface Area Micro-Mesoporous Graphene for Electrochemical Applications. *Sci. Rep.* **2021**, *11*, 22054. [[CrossRef](#)] [[PubMed](#)]
27. Lu, H.; Gan, X.; Jia, B.; Mao, D.; Zhao, J. Tunable High-Efficiency Light Absorption of Monolayer Graphene via Tamm Plasmon Polaritons. *Opt. Lett.* **2016**, *41*, 4743–4746. [[CrossRef](#)] [[PubMed](#)]
28. Kim, S.J.; Choi, K.; Lee, B.; Kim, Y.; Hong, B.H. Materials for Flexible, Stretchable Electronics: Graphene and 2D Materials. *Annu. Rev. Mater. Res.* **2015**, *45*, 63–84. [[CrossRef](#)]
29. Catania, F.; Marras, E.; Giorcelli, M.; Jagdale, P.; Lavagna, L.; Tagliaferro, A.; Bartoli, M. A Review on Recent Advancements of Graphene and Graphene-Related Materials in Biological Applications. *Appl. Sci.* **2021**, *11*, 614. [[CrossRef](#)]
30. Reghunath, R.; Devi, K.; Singh, K.K. Recent Advances in Graphene Based Electrochemical Glucose Sensor. *Nano-Struct. Nano-Objects* **2021**, *26*, 100750. [[CrossRef](#)]
31. Arumugasamy, S.K.; Govindaraju, S.; Yun, K. Electrochemical Sensor for Detecting Dopamine Using Graphene Quantum Dots Incorporated with Multiwall Carbon Nanotubes. *Appl. Surf. Sci.* **2020**, *508*, 145294. [[CrossRef](#)]
32. Wu, S.; Jiang, M.; Mao, H.; Zhao, N.; He, D.; Chen, Q.; Liu, D.; Zhang, W.; Song, X.-M. A Sensitive Cholesterol Electrochemical Biosensor Based on Biomimetic Cerasome and Graphene Quantum Dots. *Anal. Bioanal. Chem.* **2022**, *414*, 3593–3603. [[CrossRef](#)]
33. Wang, C.-F.; Sun, X.-Y.; Su, M.; Wang, Y.-P.; Lv, Y.-K. Electrochemical Biosensors Based on Antibody, Nucleic Acid and Enzyme Functionalized Graphene for the Detection of Disease-Related Biomolecules. *Analyst* **2020**, *145*, 1550–1562. [[CrossRef](#)] [[PubMed](#)]
34. Fritea, L.; Tertis, M.; Sandulescu, R.; Cristea, C. Chapter Eleven—Enzyme–Graphene Platforms for Electrochemical Biosensor Design With Biomedical Applications. In *Methods in Enzymology*; Kumar, C.V., Ed.; Enzyme Nanoarchitectures: Enzymes Armored with Graphene; Academic Press: Cambridge, MA, USA, 2018; Volume 609, pp. 293–333.
35. Bai, Y.; Xu, T.; Zhang, X. Graphene-Based Biosensors for Detection of Biomarkers. *Micromachines* **2020**, *11*, 60. [[CrossRef](#)] [[PubMed](#)]
36. Georgakilas, V.; Otyepka, M.; Bourlinos, A.B.; Chandra, V.; Kim, N.; Kemp, K.C.; Hobza, P.; Zboril, R.; Kim, K.S. Functionalization of Graphene: Covalent and Non-Covalent Approaches, Derivatives and Applications. *Chem. Rev.* **2012**, *112*, 6156–6214. [[CrossRef](#)] [[PubMed](#)]
37. Guo, S.; Raya, J.; Ji, D.; Nishina, Y.; Ménard-Moyon, C.; Bianco, A. Is Carboxylation an Efficient Method for Graphene Oxide Functionalization? *Nanoscale Adv.* **2020**, *2*, 4085–4092. [[CrossRef](#)] [[PubMed](#)]
38. Sierra, U.; Cuara, E.; Mercado, A.; Díaz-Barriga, E.; Bahena, A.; Cortés, A.; Martínez, J.P.; Solà, M.; Fernández, S. Efficient Synthesis of Amine-Functionalized Graphene Oxide by Ultrasound-Assisted Reactions and Density Functional Theory Mechanistic Insight. *Appl. Nanosci.* **2021**, *11*, 1637–1649. [[CrossRef](#)]
39. Cao, Y.; Wang, P.; Fan, J.; Yu, H. Covalently Functionalized Graphene by Thiourea for Enhancing H₂-Evolution Performance of TiO₂ Photocatalyst. *Ceram. Int.* **2021**, *47*, 654–661. [[CrossRef](#)]
40. Yu, W.; Sisi, L.; Haiyan, Y.; Jie, L. Progress in the Functional Modification of Graphene/Graphene Oxide: A Review. *RSC Adv.* **2020**, *10*, 15328–15345. [[CrossRef](#)]
41. Georgakilas, V.; Tiwari, J.N.; Kemp, K.C.; Perman, J.A.; Bourlinos, A.B.; Kim, K.S.; Zboril, R. Noncovalent Functionalization of Graphene and Graphene Oxide for Energy Materials, Biosensing, Catalytic, and Biomedical Applications. *Chem. Rev.* **2016**, *116*, 5464–5519. [[CrossRef](#)] [[PubMed](#)]
42. Lin, H.-Y.; Chen, W.-H.; Huang, C.-H. Chapter 15—Graphene in Electrochemical Biosensors. In *Biomedical Applications of Graphene and 2D Nanomaterials*; Nurunnabi, M., McCarthy, J.R., Eds.; Micro and Nano Technologies; Elsevier: Amsterdam, The Netherlands, 2019; pp. 321–336. ISBN 978-0-12-815889-0.
43. Perreault, F.; Faria, A.F.d.; Elimelech, M. Environmental Applications of Graphene-Based Nanomaterials. *Chem. Soc. Rev.* **2015**, *44*, 5861–5896. [[CrossRef](#)]
44. Gosai, A.; Khondakar, K.R.; Ma, X.; Ali, M.A. Application of Functionalized Graphene Oxide Based Biosensors for Health Monitoring: Simple Graphene Derivatives to 3D Printed Platforms. *Biosensors* **2021**, *11*, 384. [[CrossRef](#)]
45. Peña-Bahamonde, J.; Nguyen, H.N.; Fanourakis, S.K.; Rodrigues, D.F. Recent Advances in Graphene-Based Biosensor Technology with Applications in Life Sciences. *J. Nanobiotechnol.* **2018**, *16*, 75. [[CrossRef](#)] [[PubMed](#)]
46. Lee, J.-H.; Park, S.-J.; Choi, J.-W. Electrical Property of Graphene and Its Application to Electrochemical Biosensing. *Nanomaterials* **2019**, *9*, 297. [[CrossRef](#)] [[PubMed](#)]
47. Sengupta, J.; Hussain, C.M. Graphene-Based Field-Effect Transistor Biosensors for the Rapid Detection and Analysis of Viruses: A Perspective in View of COVID-19. *Carbon. Trends* **2021**, *2*, 100011. [[CrossRef](#)]
48. Alhazmi, H.A.; Ahsan, W.; Mangla, B.; Javed, S.; Hassan, M.Z.; Asmari, M.; Bratty, M.A.; Najmi, A. Graphene-Based Biosensors for Disease Theranostics: Development, Applications, and Recent Advancements. *Nanotechnol. Rev.* **2022**, *11*, 96–116. [[CrossRef](#)]

49. Liang, X.; Li, N.; Zhang, R.; Yin, P.; Zhang, C.; Yang, N.; Liang, K.; Kong, B. Carbon-Based SERS Biosensor: From Substrate Design to Sensing and Bioapplication. *NPG Asia Mater.* **2021**, *13*, 1–36. [[CrossRef](#)]
50. Sengupta, J.; Adhikari, A.; Hussain, C.M. Graphene-Based Analytical Lab-on-Chip Devices for Detection of Viruses: A Review. *Carbon. Trends* **2021**, *4*, 100072. [[CrossRef](#)]
51. Ansari, A.A.; Malhotra, B.D. Current Progress in Organic–Inorganic Hetero-Nano-Interfaces Based Electrochemical Biosensors for Healthcare Monitoring. *Coord. Chem. Rev.* **2022**, *452*, 214282. [[CrossRef](#)]
52. Erdem, A.; Senturk, H.; Yildiz, E.; Maral, M. Amperometric Immunosensor Developed for Sensitive Detection of SARS-CoV-2 Spike S1 Protein in Combined with Portable Device. *Talanta* **2022**, *244*, 123422. [[CrossRef](#)] [[PubMed](#)]
53. Ghanam, A.; Mohammadi, H.; Amine, A.; Haddour, N.; Buret, F. Chemical Sensors. In *Encyclopedia of Sensors and Biosensors*, 1st ed.; Narayan, R., Ed.; Elsevier: Oxford, UK, 2023; pp. 161–177. ISBN 978-0-12-822549-3.
54. Torrente-Rodríguez, R.M.; Lukas, H.; Tu, J.; Min, J.; Yang, Y.; Xu, C.; Rossiter, H.B.; Gao, W. SARS-CoV-2 RapidPlex: A Graphene-Based Multiplexed Telemedicine Platform for Rapid and Low-Cost COVID-19 Diagnosis and Monitoring. *Matter* **2020**, *3*, 1981–1998. [[CrossRef](#)]
55. Jaewjaroenwattana, J.; Phoolcharoen, W.; Pasomsub, E.; Teengam, P.; Chailapakul, O. Electrochemical Paper-Based Antigen Sensing Platform Using Plant-Derived Monoclonal Antibody for Detecting SARS-CoV-2. *Talanta* **2023**, *251*, 123783. [[CrossRef](#)]
56. Ali, M.A.; Hu, C.; Zhang, F.; Jahan, S.; Yuan, B.; Saleh, M.S.; Gao, S.-J.; Panat, R. N Protein-Based Ultrasensitive SARS-CoV-2 Antibody Detection in Seconds via 3D Nanoprinted, Microarchitected Array Electrodes. *J. Med. Virol.* **2022**, *94*, 2067–2078. [[CrossRef](#)] [[PubMed](#)]
57. Beduk, T.; Beduk, D.; de Oliveira Filho, J.I.; Zihnioglu, F.; Cicek, C.; Serto, R.; Arda, B.; Goksel, T.; Turhan, K.; Salama, K.N.; et al. Rapid Point-of-Care COVID-19 Diagnosis with a Gold-Nanoarchitecture-Assisted Laser-Scribed Graphene Biosensor. *Anal. Chem.* **2021**, *93*, 8585–8594. [[CrossRef](#)] [[PubMed](#)]
58. Mojsoska, B.; Larsen, S.; Olsen, D.A.; Madsen, J.S.; Brandslund, I.; Alatraktchi, F.A. Rapid SARS-CoV-2 Detection Using Electrochemical Immunosensor. *Sensors* **2021**, *21*, 390. [[CrossRef](#)] [[PubMed](#)]
59. Yang, B.; Zeng, X.; Zhang, J.; Kong, J.; Fang, X. Accurate Identification of SARS-CoV-2 Variant Delta Using Graphene/CRISPR-DCas9 Electrochemical Biosensor. *Talanta* **2022**, *249*, 123687. [[CrossRef](#)] [[PubMed](#)]
60. Damiaty, S.; Sjøpstad, S.; Peacock, M.; Akhtar, A.S.; Pinto, I.; Soares, R.R.G.; Russom, A. Flex Printed Circuit Board Implemented Graphene-Based DNA Sensor for Detection of SARS-CoV-2. *IEEE Sens. J.* **2021**, *21*, 13060–13067. [[CrossRef](#)]
61. Ji, D.; Guo, M.; Wu, Y.; Liu, W.; Luo, S.; Wang, X.; Kang, H.; Chen, Y.; Dai, C.; Kong, D.; et al. Electrochemical Detection of a Few Copies of Unamplified SARS-CoV-2 Nucleic Acids by a Self-Actuated Molecular System. *J. Am. Chem. Soc.* **2022**, *144*, 13526–13537. [[CrossRef](#)]
62. Silva, L.R.G.; Stefano, J.S.; Orzari, L.O.; Brazaca, L.C.; Carrilho, E.; Marcolino-Junior, L.H.; Bergamini, M.F.; Munoz, R.A.A.; Janegitz, B.C. Electrochemical Biosensor for SARS-CoV-2 CDNA Detection Using AuPs-Modified 3D-Printed Graphene Electrodes. *Biosensors* **2022**, *12*, 622. [[CrossRef](#)]
63. Amouzadeh Tabrizi, M.; Acedo, P. An Electrochemical Membrane-Based Aptasensor for Detection of Severe Acute Respiratory Syndrome Coronavirus-2 Receptor-Binding Domain. *Appl. Surf. Sci.* **2022**, *598*, 153867. [[CrossRef](#)]
64. Amouzadeh Tabrizi, M.; Acedo, P. Highly Sensitive Aptasensor for the Detection of SARS-CoV-2-RBD Using Aptamer-Gated Methylene Blue@mesoporous Silica Film/Laser Engraved Graphene Electrode. *Biosens. Bioelectron.* **2022**, *215*, 114556. [[CrossRef](#)]
65. Primpray, V.; Kamsong, W.; Pakapongpan, S.; Phochakum, K.; Kaewchaem, A.; Sappat, A.; Wisitsoraat, A.; Lomas, T.; Tuantranont, A.; Karuwan, C. An Alternative Ready-to-Use Electrochemical Immunosensor for Point-of-Care COVID-19 Diagnosis Using Graphene Screen-Printed Electrodes Coupled with a 3D-Printed Portable Potentiostat. *Talanta Open.* **2022**, *6*, 100155. [[CrossRef](#)]
66. Kumar, T.H.V.; Srinivasan, S.; Krishnan, V.; Vaidyanathan, R.; Babu, K.A.; Natarajan, S.; Veerapandian, M. Peptide-Based Direct Electrochemical Detection of Receptor Binding Domains of SARS-CoV-2 Spike Protein in Pristine Samples. *Sens. Actuators B Chem.* **2023**, *377*, 133052. [[CrossRef](#)] [[PubMed](#)]
67. Liv, L.; Çoban, G.; Nakiboğlu, N.; Kocagöz, T. A Rapid, Ultrasensitive Voltammetric Biosensor for Determining SARS-CoV-2 Spike Protein in Real Samples. *Biosens. Bioelectron.* **2021**, *192*, 113497. [[CrossRef](#)] [[PubMed](#)]
68. Hashemi, S.A.; Golab Behbahan, N.G.; Bahrani, S.; Mousavi, S.M.; Gholami, A.; Ramakrishna, S.; Firoozsani, M.; Moghadami, M.; Lankarani, K.B.; Omidifar, N. Ultra-Sensitive Viral Glycoprotein Detection NanoSystem toward Accurate Tracing SARS-CoV-2 in Biological/Non-Biological Media. *Biosens. Bioelectron.* **2021**, *171*, 112731. [[CrossRef](#)] [[PubMed](#)]
69. Zhao, H.; Liu, F.; Xie, W.; Zhou, T.-C.; OuYang, J.; Jin, L.; Li, H.; Zhao, C.-Y.; Zhang, L.; Wei, J.; et al. Ultrasensitive Supersandwich-Type Electrochemical Sensor for SARS-CoV-2 from the Infected COVID-19 Patients Using a Smartphone. *Sens. Actuators B Chem.* **2021**, *327*, 128899. [[CrossRef](#)]
70. Sadique, M.A.; Yadav, S.; Ranjan, P.; Khan, R.; Khan, F.; Kumar, A.; Biswas, D. Highly Sensitive Electrochemical Immunosensor Platforms for Dual Detection of SARS-CoV-2 Antigen and Antibody Based on Gold Nanoparticle Functionalized Graphene Oxide Nanocomposites. *ACS Appl. Bio. Mater.* **2022**, *5*, 2421–2430. [[CrossRef](#)]
71. Yakoh, A.; Pimpitak, U.; Rengpipat, S.; Hirankarn, N.; Chailapakul, O.; Chaiyo, S. Paper-Based Electrochemical Biosensor for Diagnosing COVID-19: Detection of SARS-CoV-2 Antibodies and Antigen. *Biosens. Bioelectron.* **2021**, *176*, 112912. [[CrossRef](#)]
72. Liv, L.; Baş, A. Discriminative Electrochemical Biosensing of Wildtype and Omicron Variant of SARS-CoV-2 Nucleocapsid Protein with Single Platform. *Anal. Biochem.* **2022**, *657*, 114898. [[CrossRef](#)]

73. El-Said, W.A.; Al-Bogami, A.S.; Alshitari, W. Synthesis of Gold Nanoparticles@reduced Porous Graphene-Modified ITO Electrode for Spectroelectrochemical Detection of SARS-CoV-2 Spike Protein. *Spectrochim. Acta Part. A Mol. Biomol. Spectrosc.* **2022**, *264*, 120237. [[CrossRef](#)]
74. Braz, B.A.; Hospinal-Santiani, M.; Martins, G.; Pinto, C.S.; Zarbin, A.J.G.; Beirão, B.C.B.; Thomaz-Soccol, V.; Bergamini, M.F.; Marcolino-Junior, L.H.; Soccol, C.R. Graphene-Binding Peptide in Fusion with SARS-CoV-2 Antigen for Electrochemical Immunosensor Construction. *Biosensors* **2022**, *12*, 885. [[CrossRef](#)]
75. Martins, G.; Gogola, J.L.; Budni, L.H.; Papi, M.A.; Bom, M.A.T.; Budel, M.L.T.; de Souza, E.M.; Müller-Santos, M.; Beirão, B.C.B.; Banks, C.E.; et al. Novel Approach Based on GQD-PHB as Anchoring Platform for the Development of SARS-CoV-2 Electrochemical Immunosensor. *Anal. Chim. Acta* **2022**, *1232*, 340442. [[CrossRef](#)]
76. Yunus, S.; Jonas, A.M.; Lakard, B. Potentiometric Biosensors. In *Encyclopedia of Biophysics*; Roberts, G.C.K., Ed.; Springer: Berlin/Heidelberg, Germany, 2013; pp. 1941–1946. ISBN 978-3-642-16712-6.
77. Mu, L.; Chang, Y.; Sawtelle, S.D.; Wipf, M.; Duan, X.; Reed, M.A. Silicon Nanowire Field-Effect Transistors—A Versatile Class of Potentiometric Nanobiosensors. *IEEE Access* **2015**, *3*, 287–302. [[CrossRef](#)]
78. Alireza Hashemi, S.; Bahrani, S.; Mojtaba Mousavi, S.; Omidifar, N.; Ghaleh Golab Behbahan, N.; Arjmand, M.; Ramakrishna, S.; Bagheri Lankarani, K.; Moghadami, M.; Shokripour, M.; et al. Ultra-Precise Label-Free Nanosensor Based on Integrated Graphene with Au Nanostars toward Direct Detection of IgG Antibodies of SARS-CoV-2 in Blood. *J. Electroanal. Chem.* **2021**, *894*, 115341. [[CrossRef](#)]
79. Li, Y.; Peng, Z.; Holl, N.J.; Hassan, M.R.; Pappas, J.M.; Wei, C.; Izadi, O.H.; Wang, Y.; Dong, X.; Wang, C.; et al. MXene–Graphene Field-Effect Transistor Sensing of Influenza Virus and SARS-CoV-2. *ACS Omega* **2021**, *6*, 6643–6653. [[CrossRef](#)] [[PubMed](#)]
80. Seo, G.; Lee, G.; Kim, M.J.; Baek, S.-H.; Choi, M.; Ku, K.B.; Lee, C.-S.; Jun, S.; Park, D.; Kim, H.G.; et al. Rapid Detection of COVID-19 Causative Virus (SARS-CoV-2) in Human Nasopharyngeal Swab Specimens Using Field-Effect Transistor-Based Biosensor. *ACS Nano* **2020**, *14*, 5135–5142. [[CrossRef](#)] [[PubMed](#)]
81. Novodchuk, I.; Kayaharman, M.; Prassas, I.; Soosaipillai, A.; Karimi, R.; Goldthorpe, I.A.; Abdel-Rahman, E.; Sanderson, J.; Diamandis, E.P.; Bajcsy, M.; et al. Electronic Field Effect Detection of SARS-CoV-2 N-Protein before the Onset of Symptoms. *Biosens. Bioelectron.* **2022**, *210*, 114331. [[CrossRef](#)] [[PubMed](#)]
82. Wasfi, A.; Awwad, F.; Qamhieh, N.; Al Murshidi, B.; Palakkott, A.R.; Gelovani, J.G. Real-Time COVID-19 Detection via Graphite Oxide-Based Field-Effect Transistor Biosensors Decorated with Pt/Pd Nanoparticles. *Sci. Rep.* **2022**, *12*, 18155. [[CrossRef](#)]
83. Krsihna, B.V.; Ahmadsaidulu, S.; Teja, S.S.T.; Jayanthi, D.; Navaneetha, A.; Reddy, P.R.; Prakash, M.D. Design and Development of Graphene FET Biosensor for the Detection of SARS-CoV-2. *Silicon* **2022**, *14*, 5913–5921. [[CrossRef](#)]
84. Li, J.; Wu, D.; Yu, Y.; Li, T.; Li, K.; Xiao, M.-M.; Li, Y.; Zhang, Z.-Y.; Zhang, G.-J. Rapid and Unamplified Identification of COVID-19 with Morpholino-Modified Graphene Field-Effect Transistor Nanosensor. *Biosens. Bioelectron.* **2021**, *183*, 113206. [[CrossRef](#)]
85. Jang, H.-J.; Sui, X.; Zhuang, W.; Huang, X.; Chen, M.; Cai, X.; Wang, Y.; Ryu, B.; Pu, H.; Ankenbruck, N.; et al. Remote Floating-Gate Field-Effect Transistor with 2-Dimensional Reduced Graphene Oxide Sensing Layer for Reliable Detection of SARS-CoV-2 Spike Proteins. *ACS Appl. Mater. Interfaces* **2022**, *14*, 24187–24196. [[CrossRef](#)]
86. Chai, C.; Oh, S.-W. Electrochemical Impedimetric Biosensors for Food Safety. *Food Sci. Biotechnol.* **2020**, *29*, 879–887. [[CrossRef](#)]
87. Kim, S.M.; Kim, J.; Yim, G.; Ahn, H.J.; Lee, M.; Kim, T.-H.; Park, C.; Min, J.; Jang, H.; Lee, T. Fabrication of a Surface-Enhanced Raman Spectroscopy-Based Analytical Method Consisting of Multifunctional DNA Three-Way Junction-Conjugated Porous Gold Nanoparticles and Au-Te Nanoworm for C-Reactive Protein Detection. *Anal. Bioanal. Chem.* **2022**, *414*, 3197–3204. [[CrossRef](#)] [[PubMed](#)]
88. Leva-Bueno, J.; Peyman, S.A.; Millner, P.A. A Review on Impedimetric Immunosensors for Pathogen and Biomarker Detection. *Med. Microbiol. Immunol.* **2020**, *209*, 343–362. [[CrossRef](#)] [[PubMed](#)]
89. Muñoz, J.; Pumera, M. 3D-Printed COVID-19 Immunosensors with Electronic Readout. *Chem. Eng. J.* **2021**, *425*, 131433. [[CrossRef](#)]
90. Ehsan, M.A.; Khan, S.A.; Rehman, A. Screen-Printed Graphene/Carbon Electrodes on Paper Substrates as Impedance Sensors for Detection of Coronavirus in Nasopharyngeal Fluid Samples. *Diagnostics* **2021**, *11*, 1030. [[CrossRef](#)] [[PubMed](#)]
91. Ali, M.A.; Zhang, G.F.; Hu, C.; Yuan, B.; Jahan, S.; Kitsios, G.D.; Morris, A.; Gao, S.-J.; Panat, R. Ultrarapid and Ultrasensitive Detection of SARS-CoV-2 Antibodies in COVID-19 Patients via a 3D-Printed Nanomaterial-Based Biosensing Platform. *J. Med. Virol.* **2022**, *94*, 5808–5826. [[CrossRef](#)]
92. Alafeef, M.; Dighe, K.; Moitra, P.; Pan, D. Rapid, Ultrasensitive, and Quantitative Detection of SARS-CoV-2 Using Antisense Oligonucleotides Directed Electrochemical Biosensor Chip. *ACS Nano* **2020**, *14*, 17028–17045. [[CrossRef](#)]
93. Pola, C.C.; Rangnekar, S.V.; Sheets, R.; Szydłowska, B.M.; Downing, J.R.; Parate, K.W.; Wallace, S.G.; Tsai, D.; Hersam, M.C.; Gomes, C.L.; et al. Aerosol-Jet-Printed Graphene Electrochemical Immunosensors for Rapid and Label-Free Detection of SARS-CoV-2 in Saliva. *2D Mater.* **2022**, *9*, 035016. [[CrossRef](#)]
94. Ang, W.L.; Lim, R.R.X.; Ambrosi, A.; Bonanni, A. Rapid Electrochemical Detection of COVID-19 Genomic Sequence with Dual-Function Graphene Nanocolloids Based Biosensor. *FlatChem* **2022**, *32*, 100336. [[CrossRef](#)]
95. Ali, M.A.; Hu, C.; Jahan, S.; Yuan, B.; Saleh, M.S.; Ju, E.; Gao, S.-J.; Panat, R. Sensing of COVID-19 Antibodies in Seconds via Aerosol Jet Nanoprinted Reduced-Graphene-Oxide-Coated 3D Electrodes. *Adv. Mater.* **2021**, *33*, 2006647. [[CrossRef](#)]
96. Zaccariotto, G.C.; Silva, M.K.L.; Rocha, G.S.; Cesarino, I. A Novel Method for the Detection of SARS-CoV-2 Based on Graphene-Impedimetric Immunosensor. *Materials* **2021**, *14*, 4230. [[CrossRef](#)]

97. Haghayegh, F.; Salahandish, R.; Hassani, M.; Sanati-Nezhad, A. Highly Stable Buffer-Based Zinc Oxide/Reduced Graphene Oxide Nanosurface Chemistry for Rapid Immunosensing of SARS-CoV-2 Antigens. *ACS Appl. Mater. Interfaces* **2022**, *14*, 10844–10855. [[CrossRef](#)] [[PubMed](#)]
98. Greben, K.; Kovalchuk, S.; Valencia, A.M.; Kirchhof, J.N.; Heeg, S.; Rietsch, P.; Reich, S.; Cocchi, C.; Eigler, S.; Bolotin, K.I. In Situ Functionalization of Graphene. *2D Mater.* **2020**, *8*, 015022. [[CrossRef](#)]
99. Schirowski, M.; Hauke, F.; Hirsch, A. Controlling the Degree of Functionalization: In-Depth Quantification and Side-Product Analysis of Diazonium Chemistry on SWCNTs. *Chem. A Eur. J.* **2019**, *25*, 12761–12768. [[CrossRef](#)] [[PubMed](#)]
100. Devasena, T.; Francis, A.P.; Ramaprabhu, S. Toxicity of Graphene: An Update. In *Reviews of Environmental Contamination and Toxicology*; de Voogt, P., Ed.; Reviews of Environmental Contamination and Toxicology; Springer International Publishing: Cham, Switzerland, 2021; Volume 259, pp. 51–76. ISBN 978-3-030-88342-3.
101. Liao, C.; Li, Y.; Tjong, S.C. Graphene Nanomaterials: Synthesis, Biocompatibility, and Cytotoxicity. *Int. J. Mol. Sci.* **2018**, *19*, 3564. [[CrossRef](#)] [[PubMed](#)]
102. Ou, L.; Song, B.; Liang, H.; Liu, J.; Feng, X.; Deng, B.; Sun, T.; Shao, L. Toxicity of Graphene-Family Nanoparticles: A General Review of the Origins and Mechanisms. *Part. Fibre Toxicol.* **2016**, *13*, 57. [[CrossRef](#)]
103. Achawi, S.; Feneou, B.; Pourchez, J.; Forest, V. Structure–Activity Relationship of Graphene-Based Materials: Impact of the Surface Chemistry, Surface Specific Area and Lateral Size on Their In Vitro Toxicity. *Nanomaterials* **2021**, *11*, 2963. [[CrossRef](#)]
104. Huang, Y.-W.; Cambre, M.; Lee, H.-J. The Toxicity of Nanoparticles Depends on Multiple Molecular and Physicochemical Mechanisms. *Int. J. Mol. Sci.* **2017**, *18*, 2702. [[CrossRef](#)]
105. Frontiñan-Rubio, J.; González, V.J.; Vázquez, E.; Durán-Prado, M. Rapid and Efficient Testing of the Toxicity of Graphene-Related Materials in Primary Human Lung Cells. *Sci. Rep.* **2022**, *12*, 7664. [[CrossRef](#)]
106. Fadeel, B.; Bussy, C.; Merino, S.; Vázquez, E.; Flahaut, E.; Mouchet, F.; Evariste, L.; Gauthier, L.; Koivisto, A.J.; Vogel, U.; et al. Safety Assessment of Graphene-Based Materials: Focus on Human Health and the Environment. *ACS Nano* **2018**, *12*, 10582–10620. [[CrossRef](#)]
107. Adhikari, A.; Sengupta, J. Toxicity of Carbon Nanomaterials. In *Environmental Applications of Carbon. Nanomaterials-Based Devices*; John Wiley & Sons, Ltd.: Hoboken, NJ, USA, 2021; pp. 147–171. ISBN 978-3-527-83097-8.
108. Sengupta, J.; Hussain, C.M. Prospective Pathways of Green Graphene-Based Lab-on-Chip Devices: The Pursuit toward Sustainability. *Microchim. Acta* **2022**, *189*, 177. [[CrossRef](#)]
109. El Messaoudi, N.; El Mouden, A.; Fernine, Y.; El Khomri, M.; Bouich, A.; Faska, N.; Ciğeroğlu, Z.; Américo-Pinheiro, J.H.P.; Jada, A.; Lacherai, A. Green Synthesis of Ag₂O Nanoparticles Using Punica Granatum Leaf Extract for Sulfamethoxazole Antibiotic Adsorption: Characterization, Experimental Study, Modeling, and DFT Calculation. *Environ. Sci. Pollut. Res.* **2022**. [[CrossRef](#)] [[PubMed](#)]
110. Wu, S.; Wang, X.; Li, Z.; Zhang, S.; Xing, F. Recent Advances in the Fabrication and Application of Graphene Microfluidic Sensors. *Micromachines* **2020**, *11*, 1059. [[CrossRef](#)] [[PubMed](#)]
111. Radhakrishnan, S.; Mathew, M.; Sekhar Rout, C. Microfluidic Sensors Based on Two-Dimensional Materials for Chemical and Biological Assessments. *Mater. Adv.* **2022**, *3*, 1874–1904. [[CrossRef](#)]
112. Wang, X.; Walt, D.R. Simultaneous Detection of Small Molecules, Proteins and MicroRNAs Using Single Molecule Arrays. *Chem. Sci.* **2020**, *11*, 7896–7903. [[CrossRef](#)] [[PubMed](#)]
113. Murray, L.P.; Baillargeon, K.R.; Bricknell, J.R.; Mace, C.R. Determination of Sample Stability for Whole Blood Parameters Using Formal Experimental Design. *Anal. Methods* **2019**, *11*, 930–935. [[CrossRef](#)]
114. Perez, V.P.; Pessoa, W.F.B.; Galvão, B.H.A.; Sousa, E.S.S.; Dejadi, N.N.; Campana, E.H.; Cavalcanti, M.G.d.S.; Cantarelli, V.V. Evaluation of Alternative RNA Extraction Methods for Detection of SARS-CoV-2 in Nasopharyngeal Samples Using the Recommended CDC Primer-Probe Set. *J. Clin. Virol. Plus* **2021**, *1*, 100032. [[CrossRef](#)]
115. de Lima, L.F.; Ferreira, A.L.; Torres, M.D.T.; de Araujo, W.R.; de la Fuente-Nunez, C. Minute-Scale Detection of SARS-CoV-2 Using a Low-Cost Biosensor Composed of Pencil Graphite Electrodes. *Proc. Natl. Acad. Sci. USA* **2021**, *118*, e2106724118. [[CrossRef](#)]
116. Islam, A.; Mukherjee, B.; Pandey, K.K.; Keshri, A.K. Ultra-Fast, Chemical-Free, Mass Production of High Quality Exfoliated Graphene. *ACS Nano* **2021**, *15*, 1775–1784. [[CrossRef](#)]
117. Sun, Z.; Hu, Y.H. Ultrafast, Low-Cost, and Mass Production of High-Quality Graphene. *Angew. Chem. Int. Ed.* **2020**, *59*, 9232–9234. [[CrossRef](#)]
118. Mbayachi, V.B.; Ndayiragije, E.; Sammani, T.; Taj, S.; Mbuta, E.R.; Khan, A.U. Graphene Synthesis, Characterization and Its Applications: A Review. *Results Chem.* **2021**, *3*, 100163. [[CrossRef](#)]
119. Hui, F.; Vajha, P.; Ji, Y.; Pan, C.; Grustan-Gutierrez, E.; Duan, H.; He, P.; Ding, G.; Shi, Y.; Lanza, M. Variability of Graphene Devices Fabricated Using Graphene Inks: Atomic Force Microscope Tips. *Surf. Coat. Technol.* **2017**, *320*, 391–395. [[CrossRef](#)]
120. Lebedev, A.A.; Davydov, V.Y.; Usachov, D.Y.; Lebedev, S.P.; Smirnov, A.N.; Levitskii, V.S.; Elisyeyev, I.A.; Alekseev, P.A.; Dunaevskiy, M.S.; Rybkin, A.G.; et al. Study of Properties and Development of Sensors Based on Graphene Films Grown on SiC (0001) by Thermal Destruction Method. *J. Phys. Conf. Ser.* **2018**, *951*, 012007. [[CrossRef](#)]
121. Zhu, Y.; Qu, B.; Andreeva, D.V.; Ye, C.; Novoselov, K.S. Graphene Standardization: The Lesson from the East. *Mater. Today* **2021**, *47*, 9–15. [[CrossRef](#)]
122. Mourdikoudis, S.; Pallares, R.M.; Thanh, N.T.K. Characterization Techniques for Nanoparticles: Comparison and Complementarity upon Studying Nanoparticle Properties. *Nanoscale* **2018**, *10*, 12871–12934. [[CrossRef](#)]

123. Sadique, M.A.; Ranjan, P.; Yadav, S.; Khan, R. Chapter 8—Advanced High-Throughput Biosensor-Based Diagnostic Approaches for Detection of Severe Acute Respiratory Syndrome-Coronavirus-2. In *Computational Approaches for Novel Therapeutic and Diagnostic Designing to Mitigate SARS-CoV-2 Infection*; Parihar, A., Khan, R., Kumar, A., Kaushik, A.K., Gohel, H., Eds.; Academic Press: Cambridge, MA, USA, 2022; pp. 147–169. ISBN 978-0-323-91172-6.
124. Venugopalan, A. COVID-19: IIT Kharagpur Researchers Come up with Portable, Low Cost and Fast Testing Device. *Economic Times*, 25 July 2020.
125. Chauhan, N.; Maekawa, T.; Kumar, D.N.S. Graphene Based Biosensors—Accelerating Medical Diagnostics to New-Dimensions. *J. Mater. Res.* **2017**, *32*, 2860–2882. [[CrossRef](#)]
126. Center for Devices and Radiological Health In Vitro Diagnostics EUAs—Antigen Diagnostic Tests for SARS-CoV-2. Available online: <https://www.fda.gov/medical-devices/coronavirus-disease-2019-covid-19-emergency-use-authorizations-medical-devices/in-vitro-diagnostics-euas-antigen-diagnostic-tests-sars-cov-2> (accessed on 11 April 2023).
127. Diagnostic Kit Evaluation. Available online: <https://www.icmr.gov.in/ckitevaluation.html> (accessed on 11 April 2023).
128. Teo, A.K.J.; Choudhury, Y.; Tan, I.B.; Cher, C.Y.; Chew, S.H.; Wan, Z.Y.; Cheng, L.T.E.; Oon, L.L.E.; Tan, M.H.; Chan, K.S.; et al. Saliva Is More Sensitive than Nasopharyngeal or Nasal Swabs for Diagnosis of Asymptomatic and Mild COVID-19 Infection. *Sci. Rep.* **2021**, *11*, 3134. [[CrossRef](#)]
129. Byrne, R.L.; Kay, G.A.; Kontogianni, K.; Aljayyousi, G.; Brown, L.; Collins, A.M.; Cuevas, L.E.; Ferreira, D.M.; Fraser, A.J.; Garrod, G.; et al. Saliva Alternative to Upper Respiratory Swabs for SARS-CoV-2 Diagnosis. *Emerg. Infect. Dis. J. CDC* **2020**, *26*, 2769–2770. [[CrossRef](#)]
130. Labbé, A.-C.; Benoit, P.; Gobeille Paré, S.; Coutlée, F.; Lévesque, S.; Bestman-Smith, J.; Dumaresq, J.; Lavallée, C.; Houle, C.; Martin, P.; et al. Comparison of Saliva with Oral and Nasopharyngeal Swabs for SARS-CoV-2 Detection on Various Commercial and Laboratory-Developed Assays. *J. Med. Virol.* **2021**, *93*, 5333–5338. [[CrossRef](#)]
131. Bastos, M.L.; Perlman-Arrow, S.; Menzies, D.; Campbell, J.R. The Sensitivity and Costs of Testing for SARS-CoV-2 Infection With Saliva Versus Nasopharyngeal Swabs. *Ann. Intern. Med.* **2021**, *174*, 501–510. [[CrossRef](#)]
132. Angcard COVID-19 Saliva Home Testing Kits. Available online: <https://www.angstrombiotech.in/angcard.html> (accessed on 11 April 2023).
133. Vogels, C.B.F.; Watkins, A.E.; Harden, C.A.; Brackney, D.E.; Shafer, J.; Wang, J.; Caraballo, C.; Kalinich, C.C.; Ott, I.M.; Fauver, J.R.; et al. SalivaDirect: A Simplified and Flexible Platform to Enhance SARS-CoV-2 Testing Capacity. *Med* **2021**, *2*, 263–280.e6. [[CrossRef](#)]
134. Xie, J.-W.; He, Y.; Zheng, Y.-W.; Wang, M.; Lin, Y.; Lin, L.-R. Diagnostic Accuracy of Rapid Antigen Test for SARS-CoV-2: A Systematic Review and Meta-analysis of 166,943 Suspected COVID-19 Patients. *Microbiol. Res.* **2022**, *265*, 127185. [[CrossRef](#)] [[PubMed](#)]
135. Olearo, F.; Nörz, D.; Heinrich, F.; Sutter, J.P.; Roedel, K.; Schultze, A.; Schulze zur Wiesch, J.; Braun, P.; Oestereich, L.; Kreuels, B.; et al. Handling and Accuracy of Four Rapid Antigen Tests for the Diagnosis of SARS-CoV-2 Compared to RT-QPCR. *J. Clin. Virol.* **2021**, *137*, 104782. [[CrossRef](#)]
136. Jegerlehner, S.; Suter-Riniker, F.; Jent, P.; Bittel, P.; Nagler, M. Diagnostic Accuracy of a SARS-CoV-2 Rapid Antigen Test in Real-Life Clinical Settings. *Int. J. Infect. Dis.* **2021**, *109*, 118–122. [[CrossRef](#)] [[PubMed](#)]
137. Arshadi, M.; Fardsanei, F.; Deihim, B.; Farshadzadeh, Z.; Nikkhahi, F.; Khalili, F.; Sotgiu, G.; Shahidi Bonjar, A.H.; Centis, R.; Migliori, G.B.; et al. Diagnostic Accuracy of Rapid Antigen Tests for COVID-19 Detection: A Systematic Review With Meta-Analysis. *Front. Med.* **2022**, *9*, 870738. [[CrossRef](#)] [[PubMed](#)]
138. Pandey, S.; Poudel, A.; Karki, D.; Thapa, J. Diagnostic Accuracy of Antigen-Detection Rapid Diagnostic Tests for Diagnosis of COVID-19 in Low-and Middle-Income Countries: A Systematic Review and Meta-Analysis. *PLoS Glob. Public Health* **2022**, *2*, e0000358. [[CrossRef](#)] [[PubMed](#)]
139. Khandker, S.S.; Nik Hashim, N.H.H.; Deris, Z.Z.; Shueb, R.H.; Islam, M.A. Diagnostic Accuracy of Rapid Antigen Test Kits for Detecting SARS-CoV-2: A Systematic Review and Meta-Analysis of 17,171 Suspected COVID-19 Patients. *J. Clin. Med.* **2021**, *10*, 3493. [[CrossRef](#)]
140. Dinnes, J.; Sharma, P.; Berhane, S.; Wyk, S.S.; Nyaaba, N.; Domen, J.; Taylor, M.; Cunningham, J.; Davenport, C.; Dittrich, S.; et al. Rapid, Point-of-care Antigen Tests for Diagnosis of SARS-CoV-2 Infection. *Cochrane Database Syst. Rev.* **2022**, 2022, CD013705. [[CrossRef](#)]

Disclaimer/Publisher’s Note: The statements, opinions and data contained in all publications are solely those of the individual author(s) and contributor(s) and not of MDPI and/or the editor(s). MDPI and/or the editor(s) disclaim responsibility for any injury to people or property resulting from any ideas, methods, instructions or products referred to in the content.